Master's Thesis

Development of high-energy density lithium metal batteries by constructing a robust SEI layer with Lithium hexafluorophosphate and lithium nitrate additives

Wonjoon Lee

School of Energy and Chemical Engineering
(Battery Science and Technology)

Ulsan National Institute of Science and Technology

2021

Development of high-energy density lithium metal batteries by constructing a robust SEI layer with Lithium hexafluorophosphate and lithium nitrate additives

Wonjoon Lee

School of Energy and Chemical Engineering
(Battery Science and Technology)

Ulsan National Institute of Science and Technology

Development of high-energy density lithium metal batteries by constructing a robust SEI layer with Lithium hexafluorophosphate and lithium nitrate additives

A thesis/dissertation submitted to
Ulsan National Institute of Science and Technology
in partial fulfillment of the
requirements for the degree of
Master of Science

Wonjoon Lee

06/11/2021

Approved by

Advisor
Nam-Soon Choi

Development of high-energy density lithium metal batteries by constructing a robust SEI layer with Lithium hexafluorophosphate and lithium nitrate additives

Wonjoon Lee

This certifies that the thesis/dissertation of Wonjoon Lee is approved.

06/11/2021

Signature

Advisor: Nam-Soon Choi

Signature

Sung-You Hong

Signature

Dong-Hwa Seo

Abstract

Li metal, having high gravitational energy density of 3,860 mAh g^{-1} and the lowest redox potential of -3.04 V (vs. SHE), is considered one of the most promising anode materials for high energy density nobel anodes in next-generation Li secondary batteries. However, some severe problems such as thermal runaway, depletion of electrolytes and loss of active materials triggered by electrochemical interfacial instability of Li limit the practical usage of thin Li metal anode (less excess Li) and causes decrease of cycling performance of the Li anode in Li metal batteries (LMBs).

To solve these challenges of development high energy density batteries, lithium hexafluorophosphate ($LiPF_6$) and lithium nitrate ($LiNO_3$) are used as F-donating additive and N-donating additive respectively to stabilize the interfacial reaction of Li metal and Ni-rich electrodes. It is verified that these additives can construct a combination of robust LiF and high ionic conductive Li_3N based solid electrolyte interphase (SEI) layer so it can suppress irreversible reactions of Li metal on the interphase. In addition, these additives can also suppress the oxidative decomposition of 1,2-dimethoxyethane (DME), form a stable cathode electrolyte interphase (CEI) and prevent structural deformation of Ni-rich cathodes when it is applied with high concentrated lithium bis(fluorosulfonyl)imide (LiFSI). As a result, our electrolyte attained 396 cycles of 80% capacity retention in high energy density Li metal battery (Li(40㎛)|$LiNi_{0.8}Co_{0.1}Mn_{0.1}O_2$) cycled with 0.9C-rate and 2.65 mAh cm^{-2}. It proved a potential of Li metal anode to be used practically and potential for development of advanced batteries with higher energy density.

Contents

List of Figures

Figure 15. Voltage profile of Li(40 ㎛) symmetric cells using 2032 coin-type cells with 1T spacer. (a) No additive, (b) 1.5% $LiPF_6$, (c) 3% $LiNO_3$, (d) 3% $LiNO_3$ + 1.5% $LiPF_6$, (e) 3% $LiNO_3$ + 3% $LiPF_6$

Figure 16. XPS analysis on Li precycled in different working. 2M LiFSI DME is used in working voltage of (a) 1V-0V and (b) 4.2V-3V.

Figure 17. Difference in electrochemical performance of no additive electrolyte (2M LiFSI DME) in NCM|Li, NCM|Cu and Li|Cu. (a) Precycle voltage profile of NCM|Li and NCM|Cu, (b) Voltage profile of Li|Cu, (c) ICEs of the electrolytes in different cells (d) Schematic diagram of reaction mechanism of organic.

Figure 18. (a) Voltage profile of NCM|Cu and NCM|Li at 0.1C-rate at 25ºC and (b) ICEs of the electrolytes. (c) Cycle performance and (d) coulombic efficiencies (CEs) of NCM|Cu and NCM|Li cycled with 0.5C-rate 3 times and cycled with 0.9C-rate at 25ºC. Li morphology of plated Li on Cu substrate. in NCM|Cu cell with 0.265 mA cm^{-2} (0.1C) and 2.65 mAh cm^{-2}. (e) No additive, (f) 1.5% $LiPF_6$, (g) 3% $LiNO_3$.

Figure 19. (a) Voltage profile of NCM|Cu cells with cathodes retrieved after precycles (0.1C-rate, 2.65 mAh cm^{-2}) in each electrolyte. The cell is precycled with 2M LiFSI DME (b) Mechanism of how oxidation decomposition of DME corrode Li metal. (c) Mechanism of improving Li reversibility by forming stable CEI and SEI which can prevent Li corrosion.

Figure 20. C 1s depth XPS spectra from 0s to 960s of Li metal anodes after precycle of NCM|Cu with (a) No additive, (b) 1.5% $LiPF_6$, (c) 3% $LiNO_3$. C 1s XPS spectra of NCM811 cathodes retrieved from NCM|Cu after precycle. (d) No additive, (e) 1.5% $LiPF_6$, (f) 3% $LiNO_3$.

Figure 21. Cycle performance of the electrolytes in NCM811|Li full cells with 2032 type coin cell. The cells are precycled with 0.1C-rate and 0.5C-rate 3times, then cycled with 0.9C-rate. (a) Voltage profile of precycles, (b) Cycle performance of the electrolytes in NCM|Li full cell and (c) CEs of the electrolytes.

Figure 22. (a) Voltage profile of the NCM|Cu precycled with 0.1C-rate with the cathodes retrieved after they are precycled in NCM|Li with each electrolyte. The NCM|Cu is precycled with 0.1C-rate with 2M LiFSI DME electrolytes. (b) ICEs and discharge capacities of the NCM|Cu cells.

Figure 23. (a) Voltage profile of NCM|Cu precycled with 0.1C-rate, (b) cycle performance of NCM|Cu cycled with 0.5C-rate 3times, then cycled with 0.9C-rate, (c) CEs of the NCM|Cu cells.

List of Tables

1. Introduction

1.1. Introduction of Li metal anodes and Ni-rich cathode

As a mobile device market gets bigger and global demand of lithium secondary batteries grows fast, the demand for next-generation batteries with higher energy density and capacity increase (**Figure 1**). However, because of theoretical limitation of conventional cathode/anode materials, diverse researchs for improvement of conventional materials and search for new materials are being conducted [1][2].

Li metal is one of the most promising anode materials due to its lowest electrochemical reduction potential (-3.040V vs. SHE), high theoretical gravitational capacity (3,860 mAh g^{-1}) derived from its low density (0.534 g^{-3}) (Figure 2). Therefore, lithium metal batteries (LMBs) which Ni-rich cathodes and Li metal anode are applied are expected to satisfy the performance of the batteries for growing electric vehicles (EVs) market

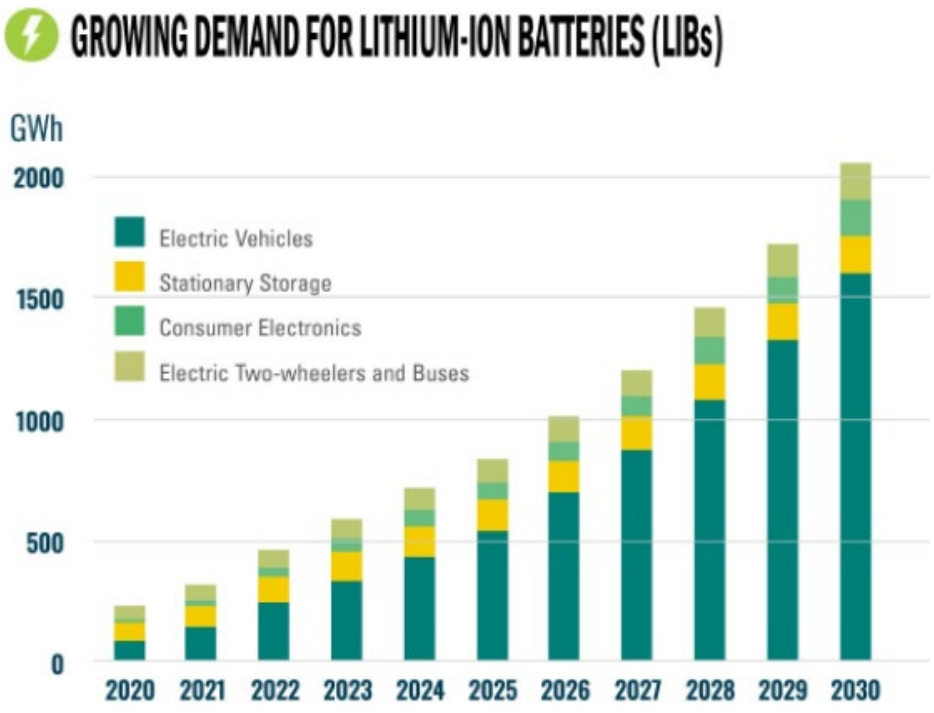

Figure 1. Growing market of LiBs for electric devices [3].

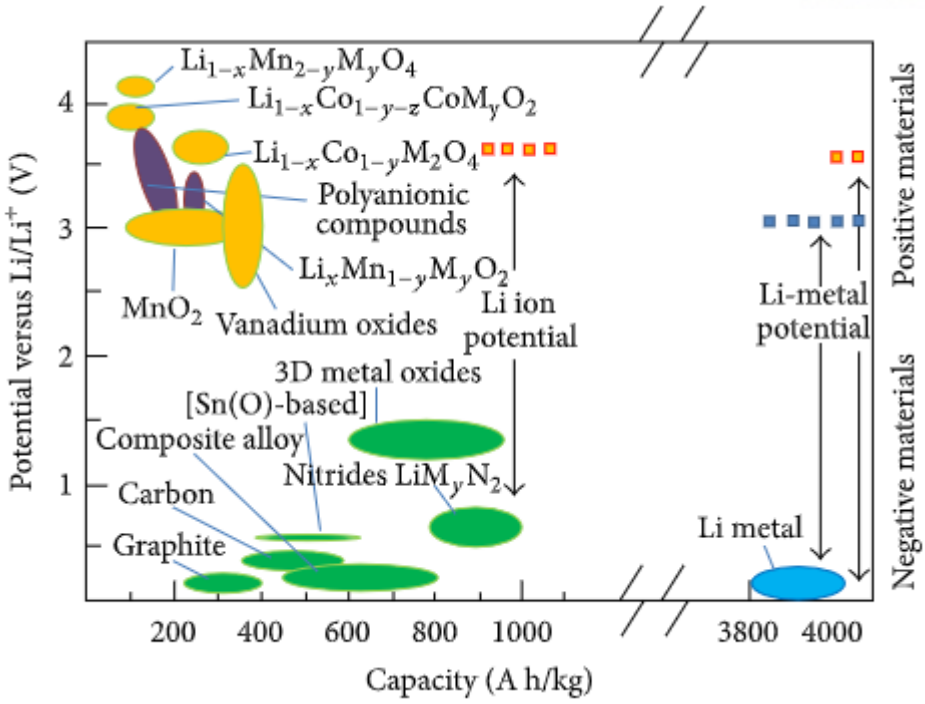

Figure 2. Theoretical capacities of diverse cathode and anode candidate materials [1].

1.2. Challenges of Li metal anodes

It is obvious that the application of Li metal anodes has significant advantages in developing advanced batteries with high-energy density. In addition, research of Li metal batteries can ultimately lead to the development of anode-free batteries which can greatly decrease the volume and cost of batteries [4]. However, some severe challenges derived from electrochemical instability of Li metal anodes prevent this novel anode from application and commercialization for advanced batteries.

1) Dendritic growth of L

The Li metal has high interfacial instability with trace gas and organic components such as electrolytes because of its low redox potential [1] and its low ionization energy [5]. It means that interphase of Li metal anode is degraded by undesirable decomposition of organic electrolytes or trace gas in the batteries and undesirable mosaic structure solid electrolyte interphase (SEI) is formed on the surface of the Li metal [6]. Then, the uneven surface derives uneven current density, so Li ions are locally plated on the anode and form irreversible Li dendrite. This dendritic growth of Li causes several problems such as capacity fading, safety problems such as internal short circuit, the formation of dead Li and continuous decomposition of electrolyte during repeated cycling [7] **(Figure 3a)**. In addition, compared

to graphite which is conventional anode, volume expansion of Li metal increases as the utilization rate of Li metal increase and SEI layer on the Li metal surface can crack during repeated cycles. Since the crack of SEI cause additional decomposition of electrolyte and more uneven SEI layer, additional dendritic growth of Li, depletion of electrolyte, formation of resistive SEI and finally decrease of cycle performance can occur.

2) Safety problems

Because of chemical instability of Li metal, trace water or oxygen trapped in the battery or formed by side reactions of electrolyte decomposition can react with Li metal forming hazardous gas such as H_2 and cause safety problems **(Figure 3b).** Even though some of the product gases formed by reaction of trace air or organic electrolyte is not flammable, they can increase the internal pressure and deform the batteries **(Figure 3c)** which lead to explosions of the batteries**.**

3) Problems on reducing excess Li

To use the strength of the Li metal and develop high energy density LMBs, the amount of excess Li should decrease to the minimum amount because it occupies significant volume, increase the weight and cost of the batteries **(Figure 4)**. However, as the excess Li decreases, the volume expansion of the Li anode during cycle increases and rest active Li which can compensate for the irreversible capacity of Li metal anode decreases. As a result, the cycle life of the high energy density LMBs with less excess Li can be worse than conventional LiBs so it is necessary to increase the reversibility of the Li metal so that it can be used with less excess Li. Ultimately, it should be able to be applied without excess Li anode, overcoming all the problems of Li metal described above.

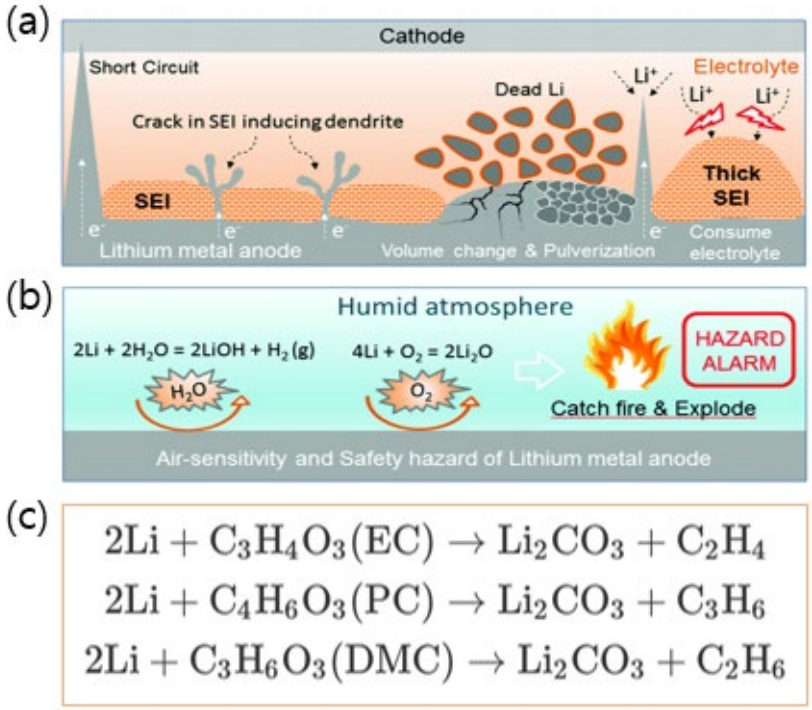

Figure 3. (a) the schematic of formation of undesirable interphase of Li metal cause by dendritic growth of Li metal; (b) undesirable interfacial reaction between trace gas and Li metal which lead to safety problem of the batteries [8]; (c) gas evolution mechanism in the Li metal batteries caused by decomposition of organic electrolytes [9].

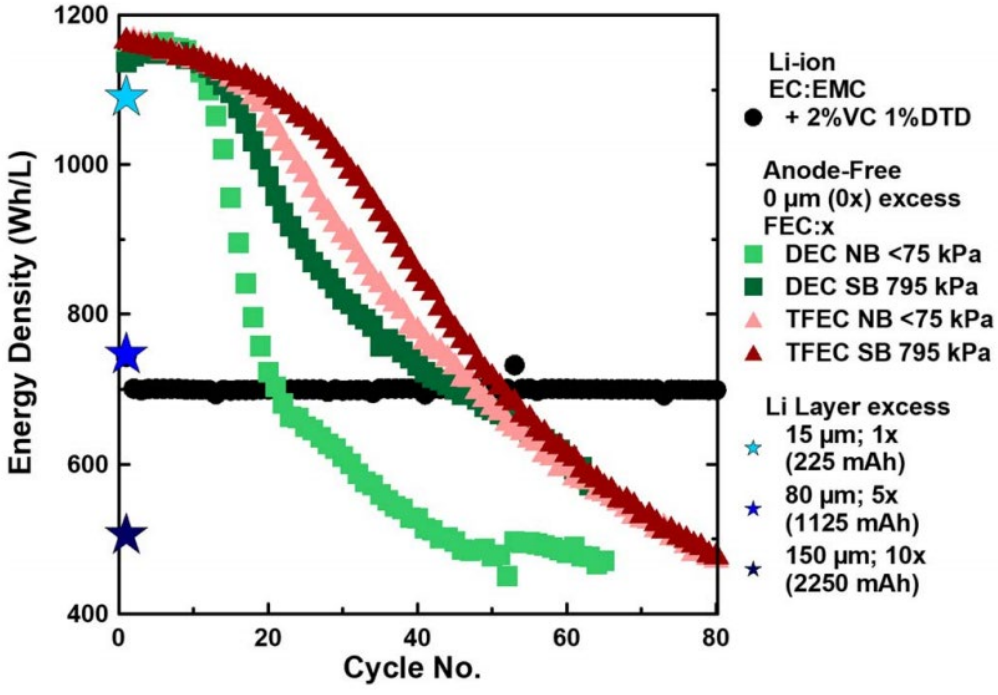

Figure 4. Energy densities of the LMBs according to its amount of excess Li [10]

1.3. Challenges of Ni-rich cathodes

To increase develop advanced batteries with higher energy density, it is also important to develop the high capacity, low costs novel cathode materials. As a cost of rare earth elements such as cobalt increase and theoretical capacities of conventional cathode materials cannot satisfy the demand anymore, Ni-rich cathodes such as NCM811, NCMA and NCA are being researched for application in the batteries. However, some severe problems derived from the increase of Ni contents occur in Ni-rich cathodes and they interrupt the commercialization of high energy density batteries.

1) Residual lithium

Because of self-reduction of the Ni from Ni^{3+} to Ni^{2+}, Li ions in the cathode react with trace gases in the batteries to adjust the charge balance of the cathodes and form residual lithium (LiOH, Li_2CO_3). The residual lithium reacts with electrolyte and form undesirable resistive SEI layers or gases.

2) Cation mixing

Since a size of the Ni^{2+} (0.69 Å) is similar to Li^+ (0.72 Å), Ni ion in the cathode can move into the Li layer, forming NiO-like phase during charging step when Ni ions are oxidized to Ni^{2+} and Li ion is delithiated. It results in a cation mixing which Ni^{2+} substitute for the Li^+ in the structure, interrupting Li ion diffusion and the lithiation of Li ions which causes irreversible capacity **(Figure 5)**.

3) Microcrack

Inhomogeneous and uneven cathode electrolyte interphase (CEI) formed by undesirable oxidative decomposition of the electrolyte can cause the localized lithiation of Li ion and localized volume expansion. This localized, anisotropic volume expansion can crack the CEI with stress and cause additional decomposition of the electrolyte, ultimately causing intergranular cracking of the particles and pulverization. This microcracking can be a reason for the decrease of energy density and the increase of gas evolution.

4) Thermal instability

In figure 6, the temperature when the phase transition of cathode occurs become lower as the Ni contents get higher. It is suggested that these phenomena are because Co ions which are located tetrahedral 8a sites makes the structure more stable in higher temperature range. Since the structural

changes of the cathodes can cause O2 gas release and increase of internal pressure, the NCM with higher Ni contents can have more safety problems in lower temperature range compared to other cathodes.

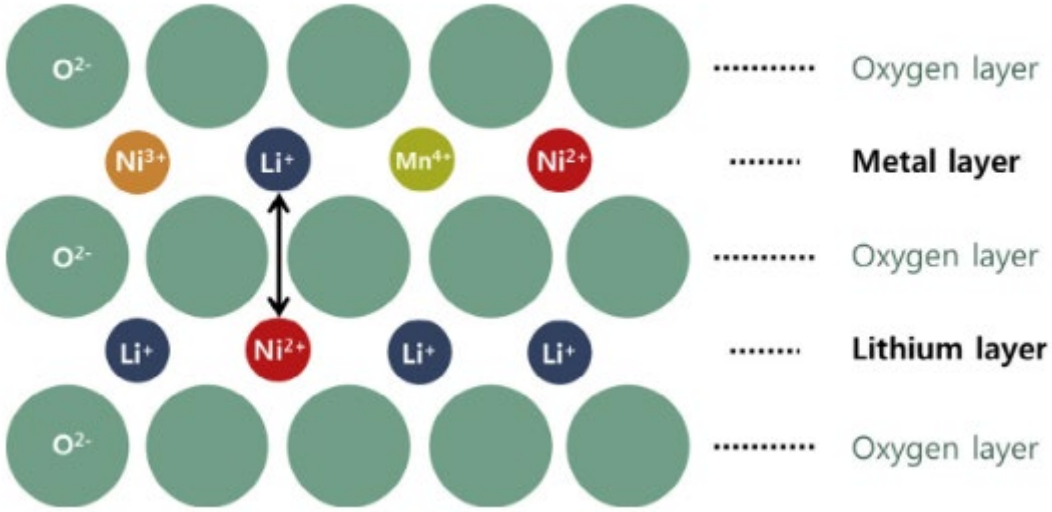

Figure 5. Schematic diagram of the cation mixing process in the NCM811 cathodes [11].

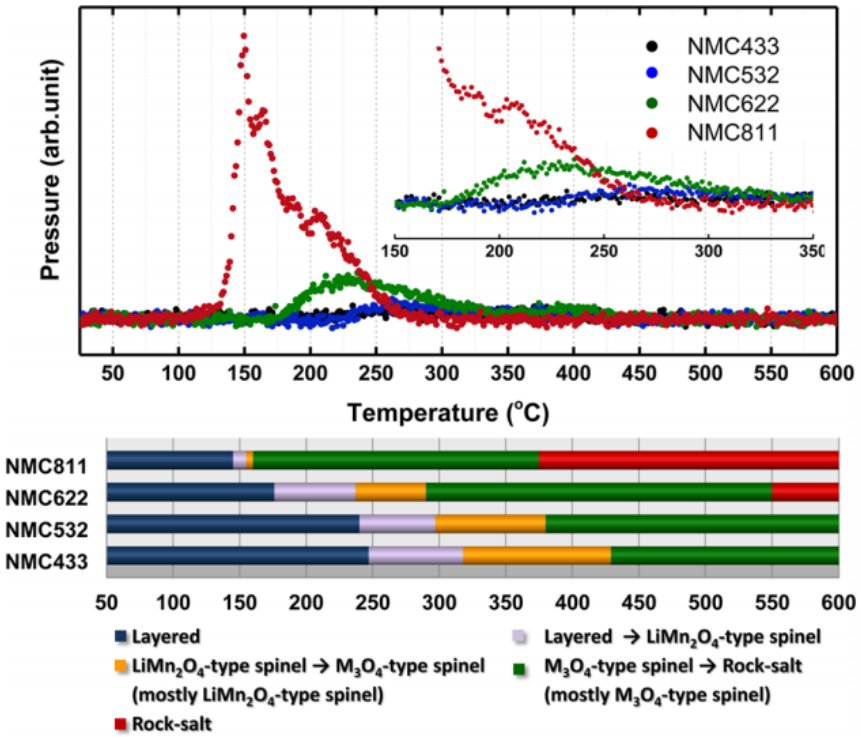

Figure 6. Temperature range of phase transition of NCM cathode with diverse Ni contents [12]

1.4. Strategies for electrolytes of LMBs

Conventional carbonated-based solvents which have been used in Li ion batteries (LIBs) are revealed that it is not appropriate to the Li metal anode because of high chemical reactivity of the solvents on the Li metal interphase [7][13]. It has reductive decomposition, forming electrochemically unstable and inhomogeneous organic-based SEI layer and causing dendritic growth of Li and inferior cycle performance. Therefore, ether solvents with electrochemical reductive reactivity with Li metal at reductive condition are widely used instead of the carbonate solvent. However, the ether solvent also has severe problems such as oxidative decomposition on the cathodes and degradation of Li metal in prolonged cycles [13][14]. As a result, it is necessary to apply specific strategies which can suppress these problems and stabilize the electrodes' interphases for long cycling.

1) Highly concentrated systems

It is reported that although ether-based electrolytes have less reactivity on Li metal, resulting in less formation of dendritic Li growth and improved reversibility of Li, it is not enough to attain good cycling performance. Aurbach and Granot reported that 1M LiTFSI with glyme solvents (1,2-dimethoxyethane, DME) shows poor cycling performance in despite of usage of relatively stable ether solvent [15]. To increase the oxidative and reductive stability of electrolytes, studies which focus on the increasing concentration of the electrolytes have been conducted [16]. Jiangfeng Qian et al. [13] showed that the electrochemical stability of ether-based electrolyte can be increased greatly when LiFSI salt is highly concentrated to 4M with DME solvent **(Figure 7)**. In highly concentrated electrolytes, DME solvent has more interaction with FSI^- anions, so the ratio of free DME decreases. As a result, it leads to improvement of electrochemical stability of the electrolytes on the interfaces, forming more stable inorganic SEI layer originated from decomposition of inorganic FSI^- anions and suppressing the oxidative decomposition of ether solvents **(Figure 8)**.

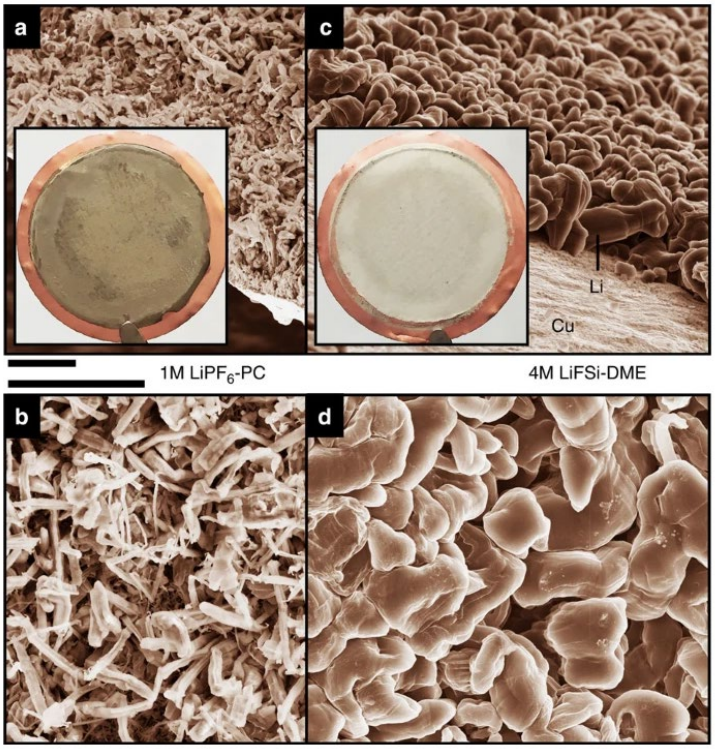

Figure 7. SEM images of Li metal after electrochemical plating on Cu substrate**.** (a,b) 1M $LiPF_6$ PC (c,d) 4M LiFSI DME. The Li is deposited with 1 mA cm^{-2} and 1.5 mAh cm^{-2}

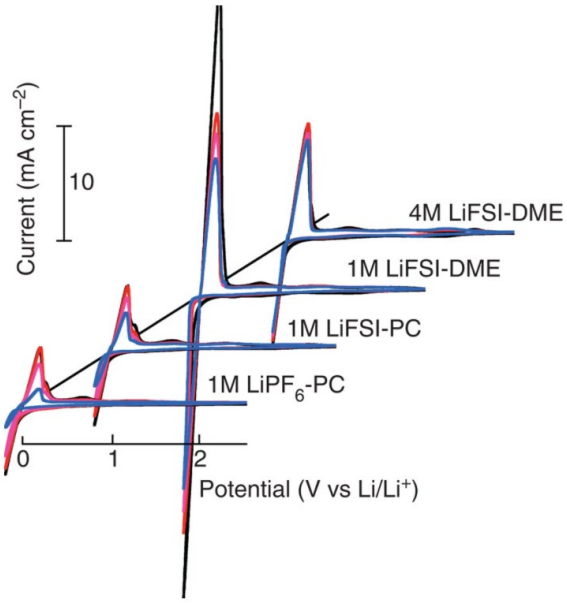

Figure 8. cyclic voltammograms of Li cycling using a PT electrode and Li metal. The scan rate was 50 mV s^{-1} [13]

2) Fluorinated solvents

It is obvious that highly concentrated electrolytes can improve the potential of the LMBs than conventional electrolytes, but the performance of the batteries is needed to be improved more because there is limitation of salt concentration in the electrolyte and high concentration causes high viscosity and costs. Not only suppressing the oxidative/reductive decomposition of the organic solvent in the electrolytes, there are also other strategies using fluorinated solvents which can form LiF-rich inorganic SEI layer as a product of their reductive decomposition. Fluorinated solvents such as 1,1,2,2-tetrafuloroethyl-2,2,3,3-tetrapropyl ether (TTE) [18] or fluorinated carbonate (FEC) [19] and bis(2,2,2-trifluoroethyl)ether (BTFE) [20] are used as co-solvent and shows meaningful stabilization effects of the co-solvents on Li metal interface, improving cycle performance and additional physical properties such as volatility and nonflammability. In addition, it is reported that the highly fluorinated solvents have diluting effect while maintaining the highly concentrated solvation structure composed of Li ions, main solvent molecules and salt anions, since the highly fluorinated solvents do not participate in solvation [20][21]. It means that if the highly fluorinated solvents are added a lot, it can take advantage of highly concentrated solvation structure of the electrolytes and low viscosity. Zhang et al. shows that application of high content of TTE can form LHCE systems **(Figure 9)** and it can greatly increase the performance of the Li metal forming stable SEI layers on Li metal anode **(Figure 10)**

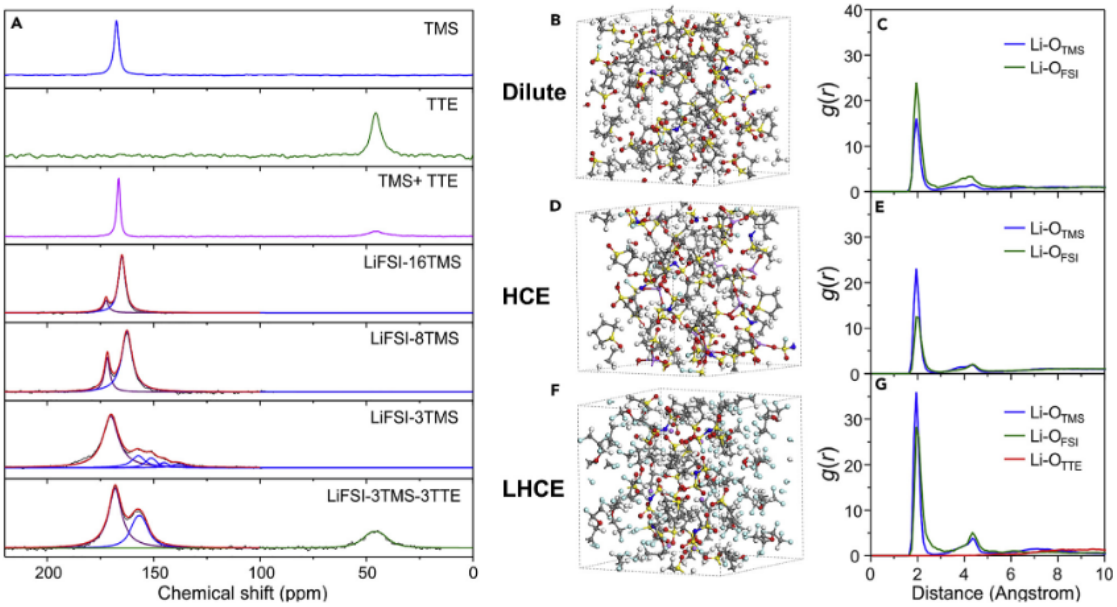

Figure 9. ^{17}O-NMR spectra, AIMD simulation and radial distribution function g(r) of the low concentrated electrolyte (Dilute), highly concentrated electrolyte (HCE) and Localized high concentrated electrolyte (LHCE) [21].

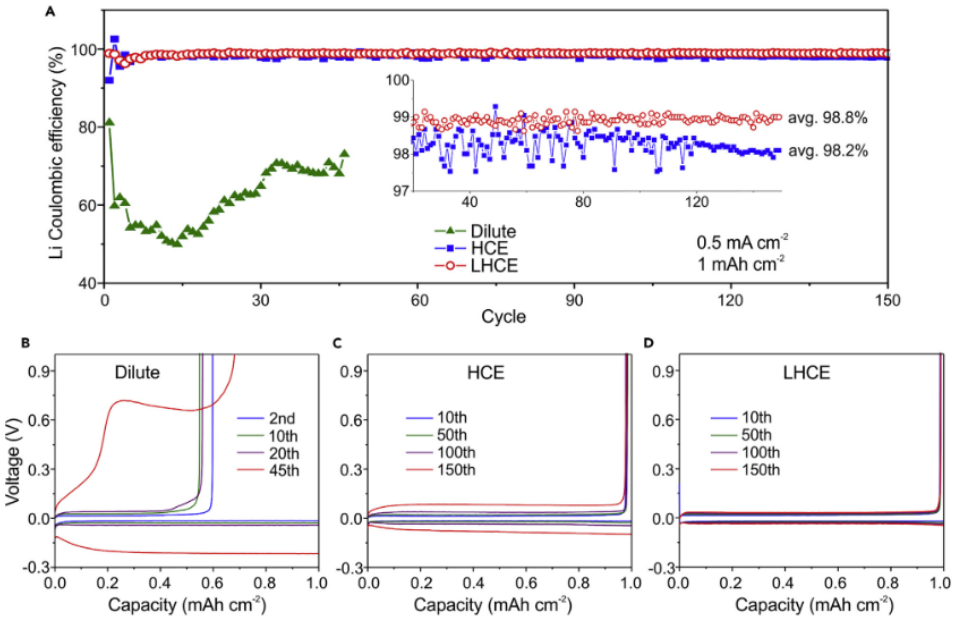

Figure 10. Cycling efficiency of Li metal in diluted electrolyte, highly concentrated electrolytes (HCE) and localized high-concentrated electrolytes (LHCE) [21]

2. Experimental

2.1. Preparation of materials (Electrolytes & Electrodes)

Electrolytes were composed of 2.0 M LiFSI (≥99.7%, Chunbo Fine Chem Co., Ltd.) in DME (≥99.9%, Sigma-Aldrich) with 3 wt% of $LiNO_3$ (≥99.9%, Sigma-Aldrich) and 1.5 wt% of $LiPF_6$(≥99.9%, Soul brain) additives and they were blended in an Ar-filled glove box where trace O_2 and H_2O contents were kept less than 1.0 ppm. For electrochemical tests, coin type cells are used. As electrodes, cathode composed of 95 wt% $LiNi_{0.8}Co_{0.2}Mn_{0.2}O_2$, 2.5 wt% denka black conducting agent, 2.5 wt% poly(vinylidene)(PVDF) binder, spread on the aluminum foil and Li metal foil (Honjo, 40 ㎛) on Cu foil are used. The cathodes were dried, pressed and then dried once more under vacuum condition at 110 °C for 10 hours for the tests. The loading level and specific capacity of the cathodes were 15.1 mg cm^{-2} and 2.65 mAh cm^{-2}, respectively. Polyethylene (PE) with the 38% porosity and 16 ㎛ thickness were used as separator.

Electrolytes	
No additive (baseline)	2M LiFSI DME
1.5% $LiPF_6$	2M LiFSI DME + 1.5% $LiPF_6$
3% $LiNO_3$	2M LiFSI DME + 3% $LiNO_3$
3% $LiNO_3$ + 1.5% $LiPF_6$	2M LiFSI DME + 3% $LiNO_3$ + 1.5% $LiPF_6$
3% $LiNO_3$ + 3% $LiPF_6$	2M LiFSI DME + 3% $LiNO_3$ + 3% $LiPF_6$
Electrodes	
Cathode	$LiNi_{0.8}Co_{0.1}Mn_{0.1}O_2$
The loading level of cathode	15.1 mg cm^{-2} (2.65 mAh cm^{-2})
Cathode composition	95.0% AM+2.5% PVDF (BM)+2.5% Denka black (CM)
Anode	40 μm foil-type Li metal

Table 1. Information about electrolytes and electrodes used in this study.

2.2. Electrochemical measurements

1) Li|NCM811 full cells

2032 coin cells with 40 μm, PE separator and NCM811 cathodes were assembled in an Ar-filled glove box. The NCM811|Li full cells were precycled at 0.1C (0.265 mA cm^{-2}) and at room temperature (25 ℃). The cells are charged to 4.2V and discharged to 3.0V. After precycle, the NCM811|Li full cells were cycled with 0.5C-rate 3 times, then cycled with 0.9C-rate. A battery measurement system (WonATech WBCS 3000) is used for electrochemical tests. For the electrochemical floating test, the cells are fully charged after precycle steps and stayed in constant voltage (CV) mode for 10 hours.

2) Li|Cu cells

2016 coin cells with 0.5T spacers or 2032 type coin cells with 1T spacers assembled with used 40 μm Li metal anode, PE separator and Cu substrate in an Ar-filled glove box. The Li|Cu cells were precycled with a 0.1C-rate with 2.65 mAh cm^{-2} at 25 ℃. After plating, Li was stripped until 1.0V *vs.* Li/Li^+.

3) Li|Li symmetric cells

2016 coin type with 40 μm Li metal anodes with 1T spacer, PE separator and 40 μm Li metal anodes were assembled in an Ar-filled glove box. The Li|Li symmetric cells were precycled with a 0.1C with 2.65 mAh cm^{-2} at 25 ℃. After precycle, the cells were cycled with a 0.5C-rate 3times then cycled with 0.9C-rate with the battery measurement system (WonATech WBCS 3000).

2.3. Characterization

To reveal the effect and mechanism of $LiPF_6$ and $LiNO_3$, electrochemically plated Li on Cu substrate in Li|Li or Li|Cu cells and electrodes precycled in NCM811|Li full cell are retrieved and rinsed with DME to remove byproducts on Li. Then surface of the retrieved electrodes was analyzed with field-emission scanning electron microscopy (FE-SEM, JSM-6700F, JEOL), ex situ X-ray photoelectron spectroscopy (XPS, Thermo Fisher Scientific Escalab 250Xi System) and time-of-flight secondary ion mass spectroscopy (TOF-SIMS) in an ultrahigh vacuum condition. FE-SEM images of the electrodes are obtained after precycle, 40 cycles and 80cycles. The cross-sectional images of the cathodes were obtained by using an ion-milling system (IM4000Plus, Hitachi). For the XPS analysis on CEI and SEI layer of the electrodes, the cells are precycled and cycled 3 times with 0.5C-rate, then retrieved. The cells are precycled, cycled 3 times with 0.5C-rate and cycled 40 times with 0.9C-rate for TOF-SIMS. Al-Kα (hν = 1486.6 eV) radiation is used for XPS analysis at a high vacuum condition and a spectrometer (ION TOF, Germany) with PIDD of 6.12 x 10^{14} ions cm^{-2} and area of 50 μm x 50 μm is used in low pressure condition (< 4.0 x 10^{-9} mbar) for TOF-SIMS analysis. Ion maps were recorded with 25 keV Bi^+ and depth profiling were recorded with a 500 eV Cs^+. After precycle and fully charging step, all cathodes were rinsed with DME and stored in reference electrolyte (2M LiFSI DME) for 1.5 day at 60 ℃.

3. Results and Discussion

3.1. Application of $LiPF_6$ and $LiNO_3$ additives

To suppress the undesirable oxidative and reductive decomposition of organic solvent DME and prevent dendritic growth of Li, it is important to form stable SEI and CEI layer with proper electrochemical properties. To increase the reversibility of Li, SEI must be able to ionic conductive and robust so that it can drive delocalized deposition of Li and suppress the volume change of the Li anode and vertical growth of Li. In **Figure 11**, it is expected that Li_3N components have high ionic conductivity which can improve reversibility of Li but it is not appropriate to be used alone because of its low electronic band gap. However, it means that if Li_3N SEI component is used with LiF component which has a low electronic band gap, it can block penetration of electrons through SEI layer and form electrochemically stable SEI layer. In addition, this Li_3N and LiF based SEI layer is expected to be robust because of their high and even Young's Modulus **(Table 2).** To form Li_3N and LiF based SEI layer, $LiNO_3$ which has been used as a SEI-forming additive in several researchs for LMBs [22][23] and $LiPF_6$ which is one of a most widely used LiF former are used as additives. Especially, $LiPF_6$ has been known for preventing Al corrosion problem which is one of the challenges of Sulfonyl based salt-ether solvent electrolytes [24][25]. In **Figure 12**, the HOMO and LUMO energy levels of electrolyte components are calculated with DFT calculations to check oxidation and reduction tendencies of the components. According to LUMO energy levels, the $LiNO_3$ and $LiPF_6$ can be reduced on the Li metal interphase prior to organic solvents, forming Li_3N and LiF in reduction reaction mechanism (**Figure 13).**

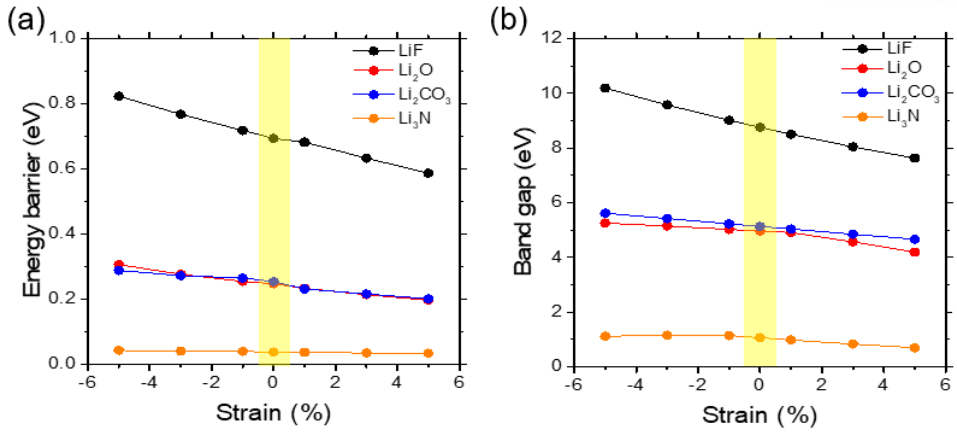

Figure 11. (a) Li migration energy and (b) electronic band gap of SEI components

(GPa)	X	Y	Z
LiF	74.3	74.3	74.3
Li_2O	199.4	199.4	199.4
Li_2CO_3	128.1	154.3	**45.9**
Li_3N	123.2	123.2	152.4

Table 2. Young's Modulus of LiF, Li_2O, Li_2CO_3, Li_3N in X,Y,Z 3D-directions.

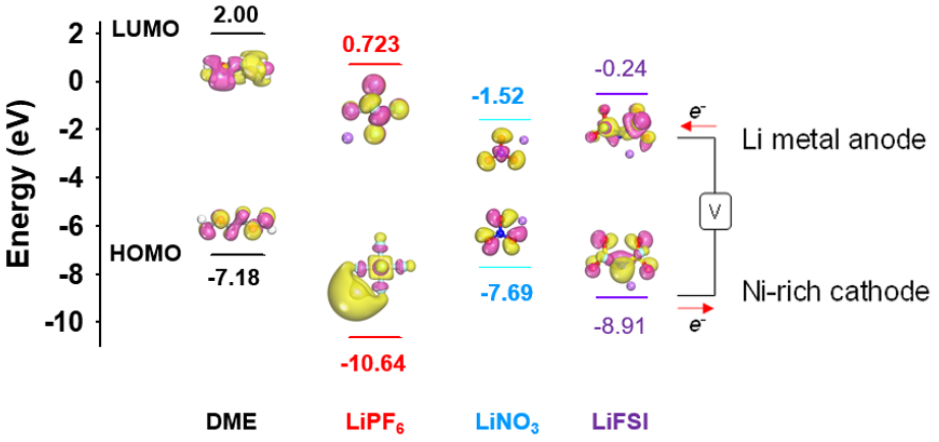

Figure 12. HOMO and LUMO energy levels of electrolyte components calculated by DFT calculation.

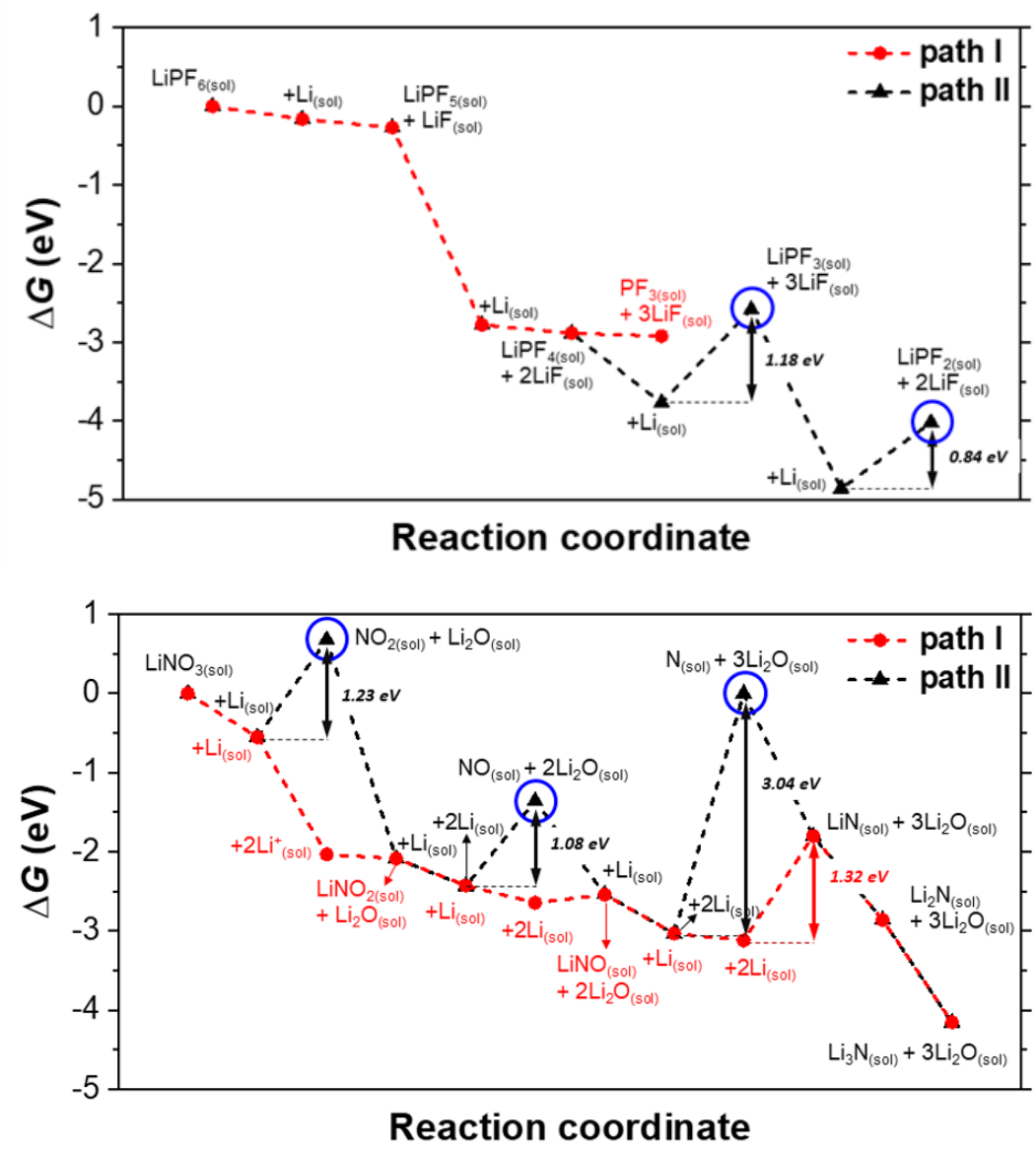

Figure 13. Interfacial reduction mechanism of $LiPF_6$ and $LiNO_3$ on the Li metal anode

3.2. Electrochemical performance of the electrolytes in Li|Cu and Li|Li cells

To examine the influence of the additives on Li reversibility, Li was electrochemically plated and stripped in Li|Cu and cycled in Li symmetric cells. Since the reversibility of Li and morphology of plated Li is significantly affected by internal pressure of the cells [26], Li plating/stripping tests in Li|Cu have conducted in 2016 coin type cells with 0.5T (0.5mm) spacers. In Figure 14a, it is shown that the Li reversibility and Coulombic efficiencies (CEs) of the cells increased as $LiPF_6$ and $LiNO_3$ additives were added respectively. In addition, Li was plated more densely in 1.5% $LiPF_6$ and 3% $LiNO_3$ electrolytes than no additive electrolyte (**Figure 14c,d,e)**. Especially, $LiNO_3$ increased the CE greatly and it seems that $LiNO_3$ improved Li reversibility and uniformity of Li plating by forming N-based ionic conductive SEI layers (**Figure 14b,e)**. When $LiNO_3$ was combined with $LiPF_6$ additive, it improved the ICE by forming robust and ionic conductive Li_3N+LiF based SEI layers. However, when $LiPF_6$ was added up to 3 wt % in the electrolyte, ICE of the cells rather decreased. It means that controlling the amount of LiF-forming additive is important to maximize the reversibility of the Li. Electrochemical performance of the electrolytes were also examined in Li|Li symmetric cells. In **Figure 15**, it is reconfirmed that $LiPF_6$ and $LiNO_3$ additives can increase the reversibility of Li in repeated cycles, and that $LiPF_6$ + $LiNO_3$ has a synergetic effect in improving the Li reversibility. While voltage of 2M LiFSI DME (No additives) started to increase at 80^{th} cycle and reached 100mV at 113^{th} cycle, $LiPF_6$, $LiNO_3$ and $LiPF_6$+$LiNO_3$ electrolytes showed more stable voltage profile for longer cycles. In addition, it is also reconfirmed that 3% $LiNO_3$ + 1.5% $LiPF_6$ electrolytes has higher Li reversibility than 3% $LiNO_3$ + 3% $LiPF_6$ electrolytes, meaning that 1.5% $LiPF_6$ is the amount of $LiPF_6$ for optimization. Based on the Li|Cu and Li|Li cell test data, it is checked whether a combination of $LiNO_3$ and $LiPF_6$ additives in LiFSI-DME based electrolyte can improve the performance of the LMBs. However, it must be pointed out that the real electrochemical condition in the practical batteries is not similar to those of Li|Cu and Li|Li cells. While working voltages of common batteries are 4V-3V, those of Li|Cu and Li|Li cells is only 1V-0V. It means that electrochemical reaction mechanism of the electrolytes in the cells are different so the results of Li|Cu and Li|Li cannot fully represent the Li reversibility in the Li metal batteries [27]. Therefore, it is necessary to examine the electrolytes in the condition which is similar to the real batteries.

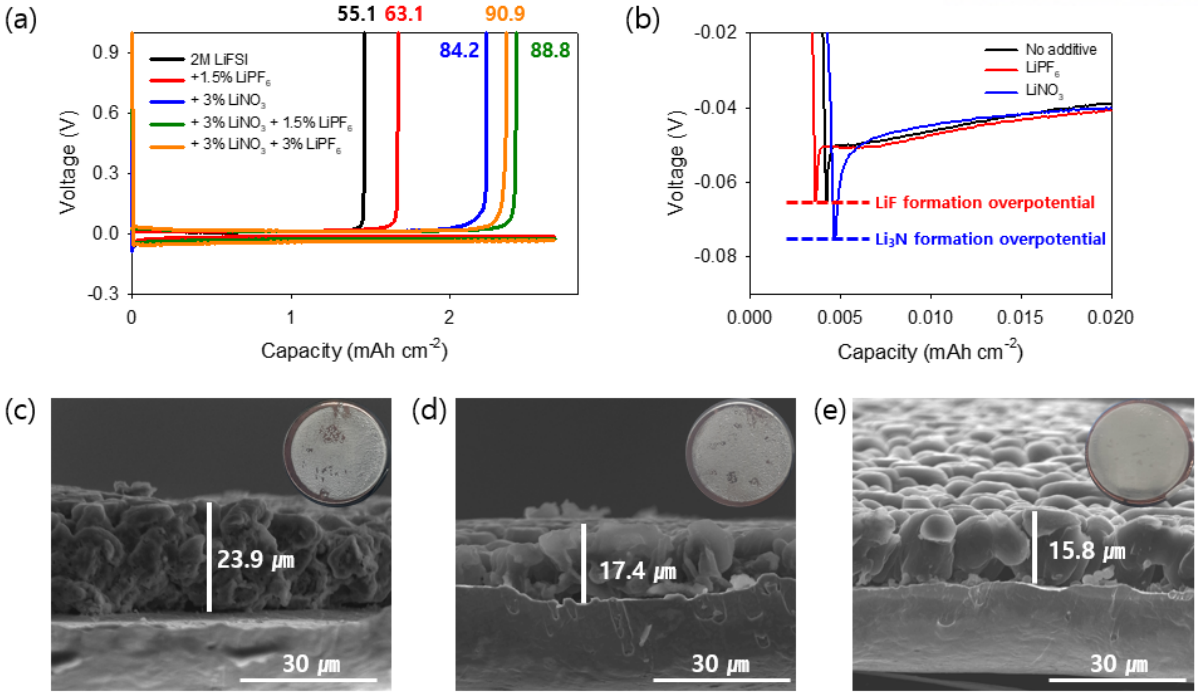

Figure 14. (a) ICEs (Initial Coulombic Efficiencies) of Li(40 ㎛)|Cu cells at 0.265 mA cm^{-2} (0.1C), 2.65 mAh cm^{-2} in 2016 type coin cell with 0.5T spacer. (b) Li plating voltage profile of 2032 type Li(40 ㎛)|Cu cells. Images of plated Li on Cu substrate retrieved from Li|Cu cells of (c) No additives, (d) 1.5% $LiPF_6$, (e) 3% $LiNO_3$.

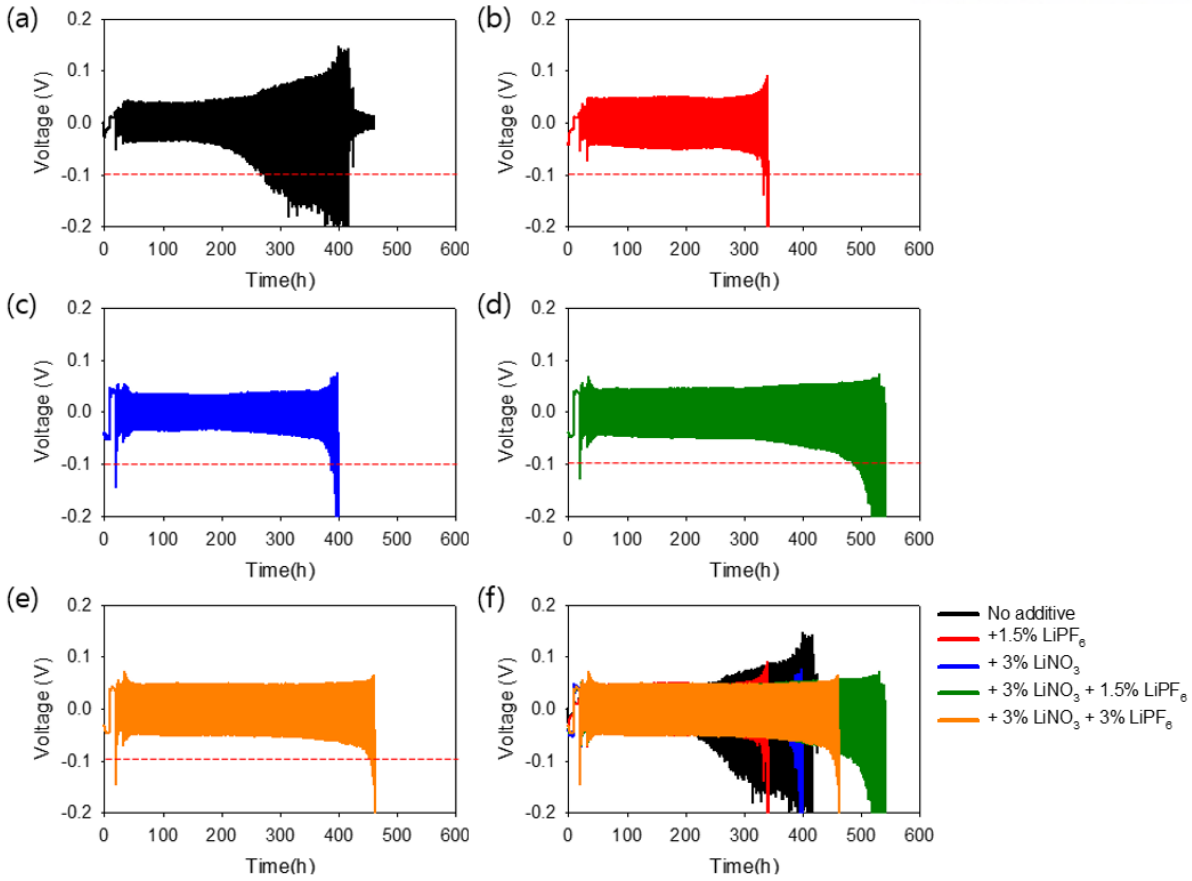

Figure 15. Voltage profile of Li(40 ㎛) symmetric cells using 2032 coin-type cells with 1T spacer. (a) No additive, (b) 1.5% $LiPF_6$, (c) 3% $LiNO_3$, (d) 3% $LiNO_3$ + 1.5% $LiPF_6$, (e) 3% $LiNO_3$ + 3% $LiPF_6$

3.3. Electrochemical performance of $LiPF_6$ and $LiNO_3$ additives in NCM|Cu and NCM|Li

NCM|Cu cells which have cathode but not anode materials are good method to test the electrolytes since the NCM|Cu cells have similar working voltages to the Li metal batteries. In fact, they belong to Li metal batteries having no excess Li metal (x0) since the cells become Li metal batteries when the cell is being charged and Li is plated on Cu substrate. In addition, NCM|Cu cycle test can provide exact CEs of the cells since there is no excess Li which can compensate for the irreversible capacity of Li anode. Matthew Genovese et al. argued that CEs of Li metal batteries with excess Li indicates only CEs of the cathode [28], so CEs of anode free battery are true CEs.

To find the exact performance and mechanism of LiFSI-DME based electrolytes in real full cell condition, XPS analysis and some electrochemical tests were conducted on the Li in different working voltages. In Figure 16, it is shown that 2M LiFSI DME electrolyte formed more LiF based inorganic SEI layer when the cell was precycled in working voltage of 1V-0V, while it formed organic based SEI layer in working voltage of 4.2V-3V. In Figure 17a-c, it is shown that without excess Li, ICE of the electrolyte decreased around 23% (88.2%→65.2%) in working voltage of 4.2V-3V since irreversible capacity of Li anode was not compensated by excess Li. However, in working voltage of 1V-0V, the irreversible capacity of the no additive electrolyte was only 5%. These XPS and ICEs results indicates that LiFSI-DME is oxidatively decomposed on the cathode first, and the unstable byproducts react with Li metal forming unstable SEI layers **(Figure 17d)**. The oxidative decomposition mechanism of 1,2-dimethoxyethane in the full cell (NCM|Li) is not revealed clearly, but it is guessed that oxygen derived from redox reactions of lattice oxygen in cathodes or trace gas can react with 1,2-dimethoxyethane.

Electrolytes with each additive were tested in NCM|Cu and NCM|Li cells. In Figure 18c,d, it is shown that no additive electrolyte had poor CEs in NCM|Cu compared to NCM|Li, which means that CEI of the cathode could not suppress the continuous oxidative decomposition of the DME in the cycles so byproducts of oxidation reaction caused irreversible reactions on Li metal anode continuously. $LiPF_6$ additive showed quite improvement of CEs in NCM|Cu and NCM|Li compared to no additive electrolyte. However, ICE of NCM|Cu was as low as no additive and it means that the oxidative decomposition of DME was not prevented in precycle and it corrodes the Li metal. Meanwhile $LiNO_3$ additive showed the great improvement of ICE and CEs in the NCM|Cu. ICE and CEs of NCM|Cu and NCM|Li of $LiNO_3$ electrolytes is similar, indicating that irreversible reactions at Li anode were effectively suppressed. It is due to good reversibility of Li in $LiNO_3$ electrolyte (**Figure 14a)**, or good CEI formed by the $LiNO_3$ electrolyte. In **Figure 19a**, the cathodes were retrieved after precycles in each electrolyte and precycled again with 0.1C-rate in no additive electrolyte. It is shown that cathode retrieved from $LiNO_3$ electrolytes showed much higher ICE, meaning that $LiNO_3$ additives could form stable CEI and SEI at the same time so it improved the reversibility of Li in the full cell condition as illustrated in **Figure 19c**. **Figure 20**, C 1s XPS spectra of Li metal and cathodes retrieved from anode free cells after precycles,

verifies that CEI of $LiNO_3$ suppressed the oxidative decomposition of organic solvent DME, and prevented Li corrosion by reactive organic byproducts. It is also verified by SEM images that $LiNO_3$ electrolyte improves Li reversibility with its dense and particle-like Li morphology (**Figure 18e,f,g)**

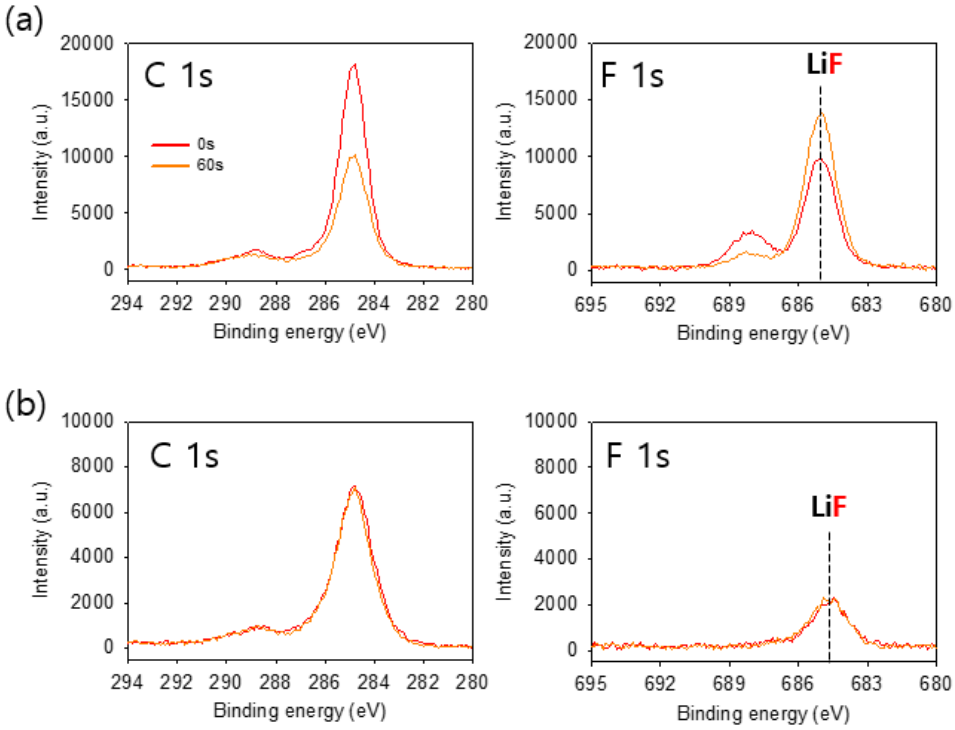

Figure 16. XPS analysis on Li precycled in different working. 2M LiFSI DME is used in working voltages of (a) 1V-0V and (b) 4.2V-3V

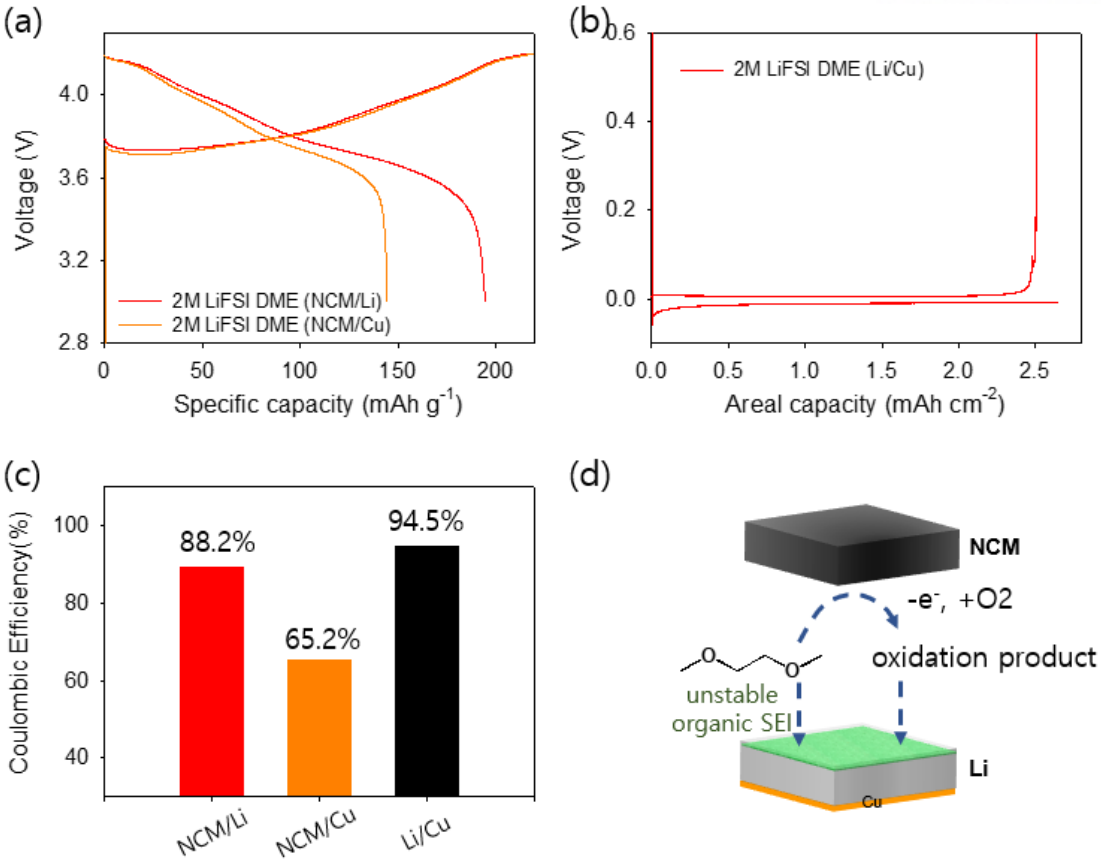

Figure 17. Difference in electrochemical performance of no additive electrolyte (2M LiFSI DME) in NCM|Li, NCM|Cu and Li|Cu. (a) Precycle voltage profile of NCM|Li and NCM|Cu, (b) Voltage profile of Li|Cu, (c) ICEs of the electrolytes in different cells (d) Schematic diagram of reaction mechanism of organic solvent in the batteries [29][30]. All tests are conducted in 0.1C-rate, 2.65 mAh cm^{-2} in 2032 type coincells.

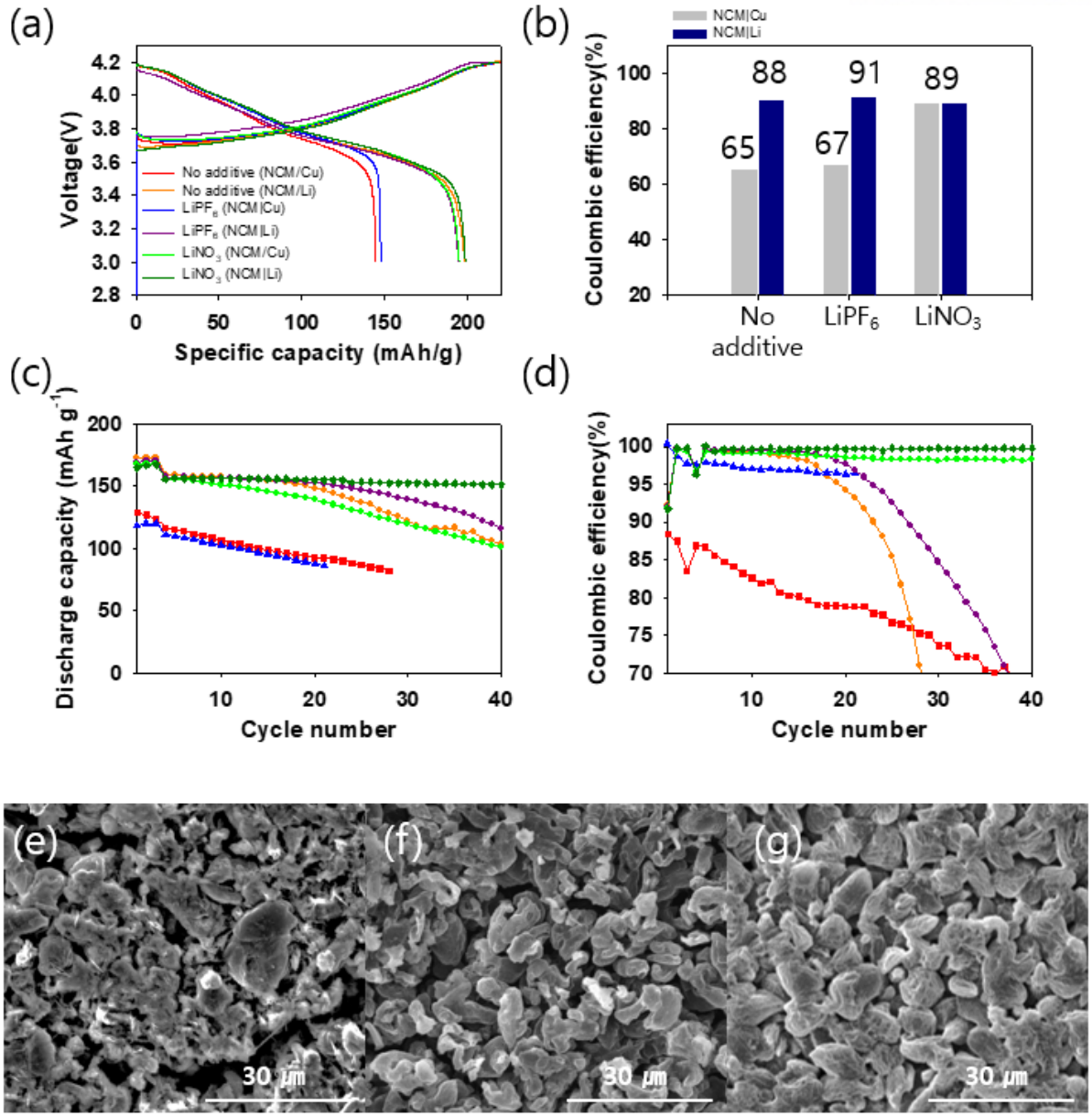

Figure 18. (a)Voltage profile of NCM|Cu and NCM|Li at 0.1C-rate at 25ºC and (b) ICEs of the electrolytes. (c) Cycle performance and (d) coulombic efficiencies (CEs) of NCM|Cu and NCM|Li cycled with 0.5C-rate 3times and cycled with 0.9C-rate at 25ºC. Li morphology of plated Li on Cu substrate in NCM|Cu cell with 0.265 mA cm^{-2} (0.1C) and 2.65 mAh cm^{-2}. (e) No additive, (f) 1.5% $LiPF_6$, (g) 3% $LiNO_3$

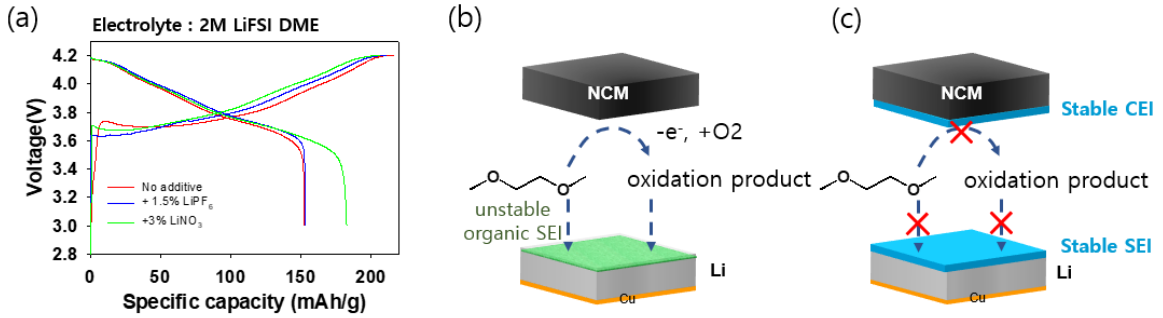

Figure 19. (a) Voltage profile of NCM|Cu cells with cathodes retrieved after precycles (0.1C-rate, 2.65 mAh cm^{-2}) in each electrolyte. The cell is precycled with 2M LiFSI DME (b) Mechanism of how oxidation decomposition of DME corrode Li metal. (c) Mechanism of improving Li reversibility by forming stable CEI and SEI which can prevent Li corrosion

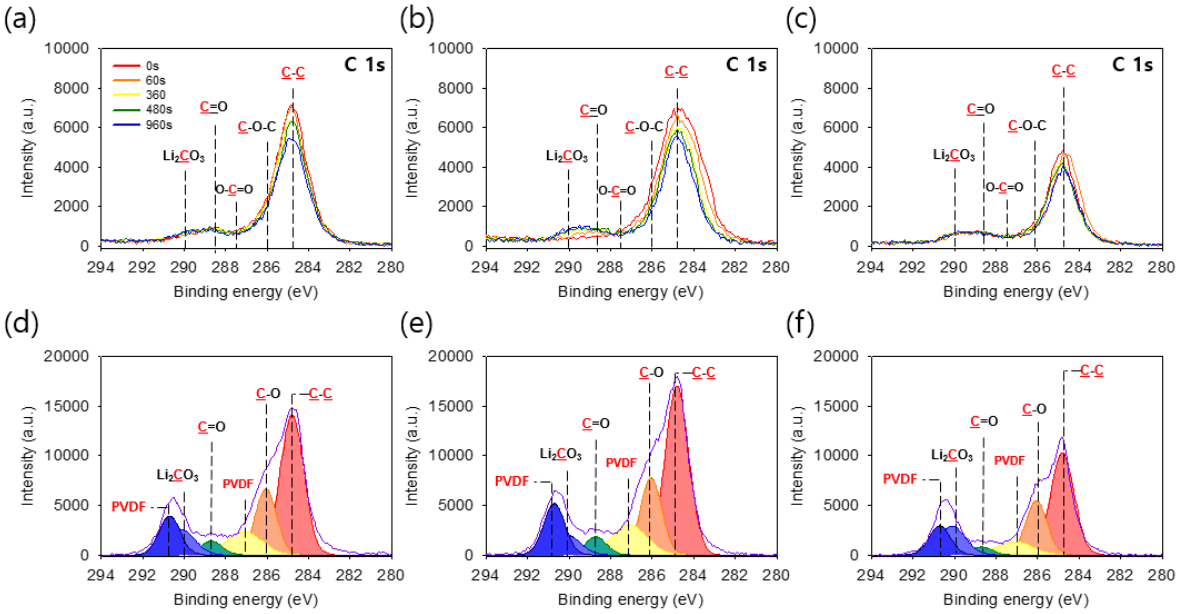

Figure 20. C 1s depth XPS spectra from 0s to 960s of Li metal anodes after precycle of NCM|Cu with (a) No additive, (b) 1.5% $LiPF_6$, (c) 3% $LiNO_3$. C 1s XPS spectra of NCM811 cathodes retrieved from NCM|Cu after precycle. (d) No additive, (e) 1.5% $LiPF_6$, (f) 3% $LiNO_3$.

3.4. Synergetic effects of $LiPF_6$ and $LiNO_3$ on electrochemical performance of NCM|Li.

It is shown that $LiNO_3$ causes the great improvement in NCM|Cu and $LiPF_6$ causes a little improvement (**Figure 18).** It may be thought that $LiPF_6$ additive is not quite necessary. However, in **Figure 15,** it is suggested that $LiPF_6$ and $LiNO_3$ additives have synergetic effects on Li anode and cathodes so it can improve the performances of the Li metal batteries.

To confirm that $LiNO_3$ and $LiPF_6$ have synergetic effects of improving the cycle performance of the Li metal batteries, the 2032 type coin cells with NCM811 cathodes (15.1 mg cm^{-2}, 2.65 mAh cm^{-2}) were assembled with 40 ㎛ Li anode and cycled with 0.9C-rate. In **Figure 21**, it is shown that the addition of $LiPF_6$ greatly improved the cycle performance of the cells, achieving 397 cycles for 80% of retention in 3% $LiNO_3$ + 1.5% $LiPF_6$. The content of 3% $LiPF_6$ rather decreased that cycle performance but still it is better than no $LiPF_6$ (+3% $LiNO_3$). It seems that +3% $LiNO_3$ +1.5% $LiPF_6$ showed the best Li reversibility in Li|Cu and LiLi cells (**Figure 14a, 15)**, so it had the best cycle performance in NCM|Li full cells based on its improved Li reversibility. However, it has to be noticed that CEs of 3% $LiNO_3$ + 3% $LiPF_6$ is higher than +3% $LiNO_3$ and +3% $LiNO_3$ + 1.5% $LiPF_6$. Since CEs of the Li metal batteries means the CEs of the cathodes [28], it can be expected that as the amount of $LiPF_6$ additive increases, the stability of cathode interphase increases. To reconfirm that CEI of the cathode gets improved as the amount of $LiPF_6$ increases, the cathodes precycled in NCM|Li with each electrolyte were retrieved and precycled again in NCM|Cu with 2M LiFSI DME electrolytes to see the ICEs of each cathode (**Figure 22)**. It is shown that the cathodes precycled with two $LiNO_3$ + $LiPF_6$ electrolytes had the highest ICE among the electrolytes and the cathode of 3% $LiNO_3$ + 3% $LiPF_6$ electrolyte had the highest discharge capacity, which means that one of the significant roles of $LiPF_6$ in $LiNO_3$ + $LiPF_6$ is to improve the stability of cathode interphase.

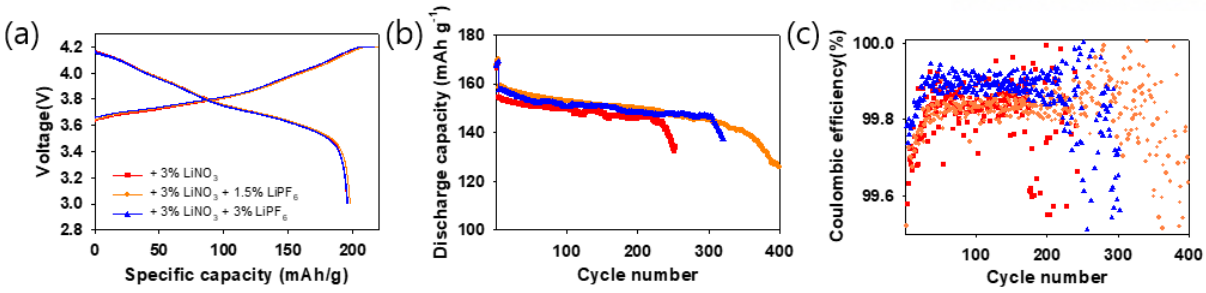

Figure 21. Cycle performance of the electrolytes in NCM811|Li full cells with 2032 type coin cell. The cells are precycled with 0.1C-rate and 0.5C-rate 3times, then cycled with 0.9C-rate. (a) Voltage profile of precycles, (b) Cycle performance of the electrolytes in NCM|Li full cell and (c) CEs of the electrolytes.

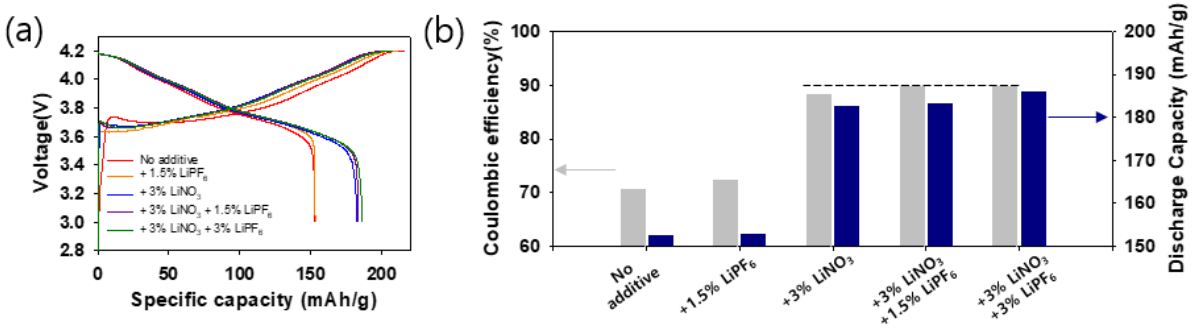

Figure 22. (a) Voltage profile of the NCM|Cu precycled with 0.1C-rate with the cathodes retrieved after they are precycled in NCM|Li with each electrolyte. The NCM|Cu is precycled with 0.1C-rate with 2M LiFSI DME electrolytes. (b) ICEs and discharge capacities of the NCM|Cu cells.

To see the exact cycle performance of the electrolyte without effect of excess Li, NCM\Cu cells were cycled with each electrolyte (**Figure 23).** It is shown that the combination of $LiNO_3$ + $LiPF_6$ increased the true CEs which consider irreversible capacities on both NCM811 cathode and Li anode, so it could improve cycle performance in anode-free (x0 excess Li) Li metal batteries. Especially, 3% $LiNO_3$ + 3% $LiPF_6$ showed the highest CEs after 25th cycles because of improved CEI performance. It must be noted that there is plateau of CEs at first few cycles and then CEs declined. Matthew Genovese et al. argued that the small

amount of Li reservoir on Cu substrate is formed in precycling step, and true CEs of the anode free batteries appear after this reservoir is completely consumed [28]. It means that the CEs decline indicates consumption of this reservoir Li metal in the cells, and the reason for higher CEs of 3% $LiNO_3$ + 1.5% $LiPF_6$ in declining region of CEs (10^{th} cycle ~ 25^{th} cycle) is that it consumed the Li reservoir more slowly because of its higher Li reversibility than that of 3% $LiNO_3$ + 3% $LiPF_6$ (**Figure 14a, 15)**.

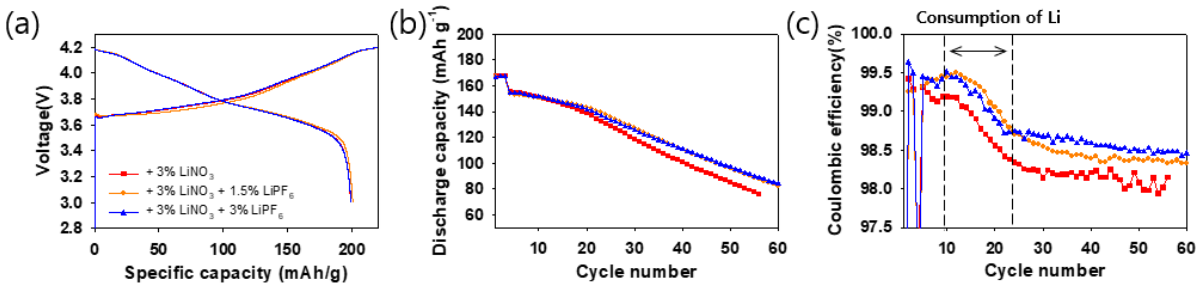

Figure 23. (a) Voltage profile of NCM|Cu precycled with 0.1C-rate, (b) cycle performance of NCM|Cu cycled with 0.5C-rate 3times, then cycled with 0.9C-rate, (c) CEs of the NCM|Cu cells.

3.5. Effect of $LiPF_6$ and $LiNO_3$ on NCM811 cathode.

It is verified that addition of $LiPF_6$ increase the stability of cathode interphase. To check the factors which causes the improvement, XPS analysis, electrochemical floating tests and linear sweep voltammetry were carried out. In **Figure 24a,** the oxidative stabilities of the electrolytes are investigated with linear sweep voltammetry at the scan rate of 1 mV s^{-1}, and it shows that $LiNO_3$ and $LiPF_6$ can improve oxidative stability of electrolyte so the $LiNO_3$ + $LiPF_6$ electrolytes have good oxidative stabilities. It should be noted that onset potential of oxidation got lower when $LiNO_3$ was added. It probably means that $LiNO_3$ was oxidatively decomposed first and it leaded to result of good CEI formation (**Figure 19)**. According to LSV test with Al|Li cells, it can be found that $LiPF_6$ can reduce oxidative current of the electrolyte because of Al passivation [25], so 3% $LiNO_3$ + 3% $LiPF_6$ has the best oxidative stability. Good oxidative stability and Al passivating ability support that $LiNO_3$ + $LiPF_6$ electrolytes (especially, 3% $LiNO_3$ + 3% $LiPF_6$) can form stable Cathode-electrolyte interphase.

In **Figure 25,** electrochemical floating tests were conducted to see stability of CEI in oxidative condition. The leakage current in No additive (2M LiFSI DME) increased after 2 hours and this phenomenon occurs due to Al corrosion. It is shown that 1.5% $LiPF_6$ can suppress this phenomenon and keep leakage current low. Based on Al passivation of $LiPF_6$ and stable CEI formation of $LiNO_3$, $LiNO_3$ + $LiPF_6$ showed the lowest leakage current after 4 hours, showing stable interphase in oxidative condition. **Figure 26** showed F 1s XPS spectra of NCM811 cathode after 3 cycles with 0.5C-rate. As more $LiPF_6$ was added, the ratio of PVDF and LiF peak increased and ratio of S-F peak decreased. The 3% $LiNO_3$ + 3% $LiPF_6$ electrolyte showed the highest LiF peak with the lowest S-F peak, which means that LiFSI decomposition was suppressed efficiently and $LiPF_6$ additives formed LiF successfully instead of LiFSI. In addition, it shows the highest PVDF peak, indicating that the thin, non-resistive CEI was formed since the decomposition of salt was suppressed. Since forming thin, non-resistive CEI formation is important to keep cathode particle electrochemically connected to each other, it was able to improve the performance of cathode in the full cells **(Figure 21c)** when $LiPF_6$ was combined with $LiNO_3$ in the electrolytes.

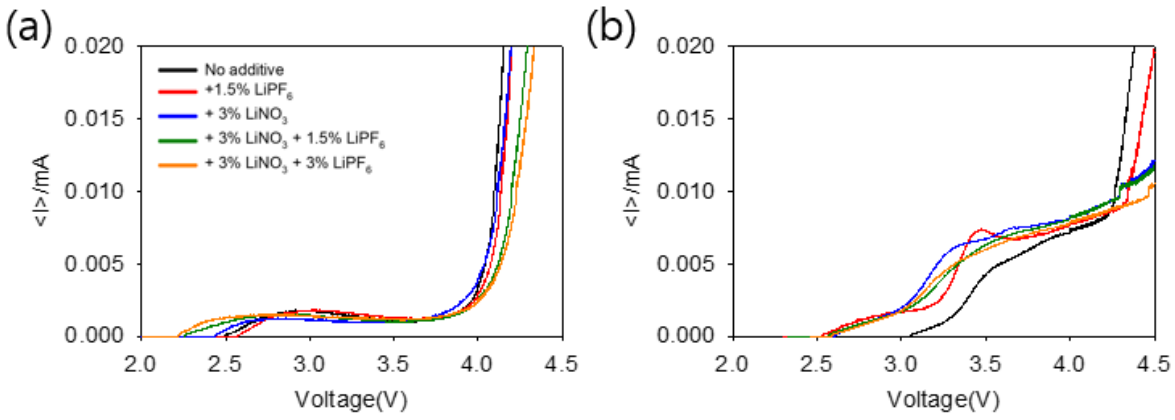

Figure 24. Oxidative stabilities of the electrolytes in (a) SUS|Li coin cells and (b) Al|Li coin cells. The test is conducted from OCV to 6V.

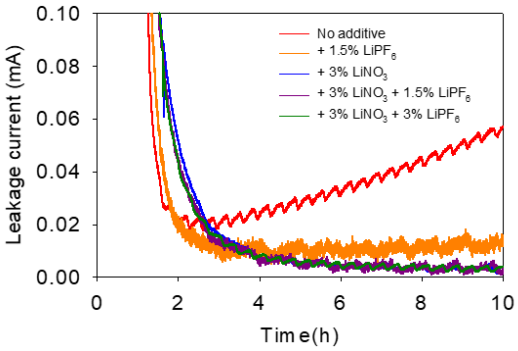

Figure 25. Floating test of NCM|Li cells for 10 hours at 4.2V. After precycle, the cell is charged to 4.2V with 0.1C-rate and keep constant voltage for 10 hours.

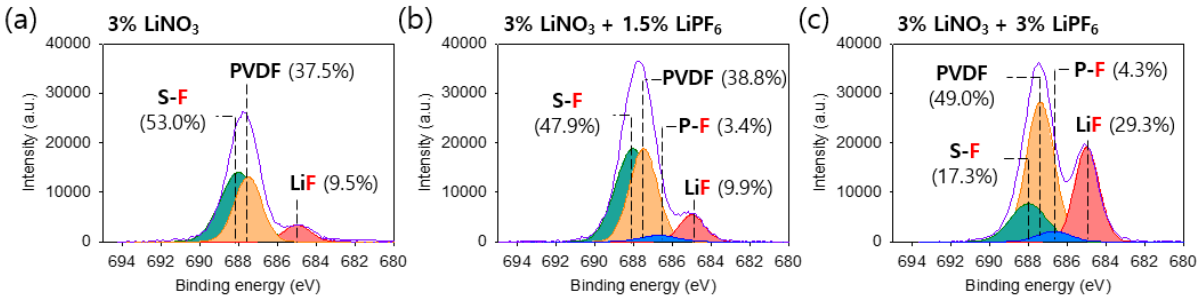

Figure 26. F 1s XPS analysis of NCM811 cathode after precycle with 0.1C-rate and cycled 3 times (0.5C-rate)

The SEM images of the cathodes retrieved after cycling with each electrolyte are shown in **Figure 27** and **Figure 28.** In **Figure 27,** it can be found that CEI layer covering NCM811 particle is very thick and the particles are severely crashed in No additive (2M LiFSI DME). It is also found that CEI layer is still thick in 1.5% $LiPF_6$ electrolyte although it is better than No additive electrolyte. In the electrolytes which contains 3% $LiNO_3$, the NCM811 particles show stable structure and no thick CEI layer. It is verified that $LiNO_3$ can stabilize the cathode. To check the difference in cathode stabilization ability between the electrolytes containing 3% $LiNO_3$, the cathodes are retrieved after 80 cycles in 3% $LiNO_3$ and 3% $LiNO_3$ + 3% $LiPF_6$ **(Figure 28)**. It is found that particles are crashed more in the 3% $LiNO_3$. As a result, as analyzed by XPS data and other electrochemical tests, it is reconfirmed that the combination of $LiPF_6$ with $LiNO_3$ can improve the stability of cathode interphase.

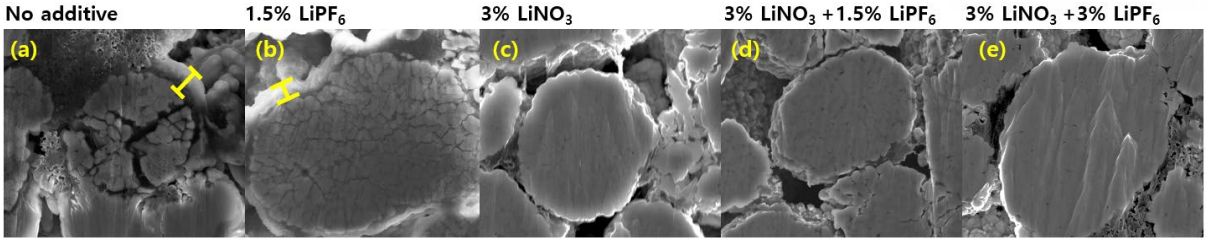

Figure 27. SEM image of cathodes cycled 40 times with each electrolyte with 0.9C-rate in NCM|Li full cell.

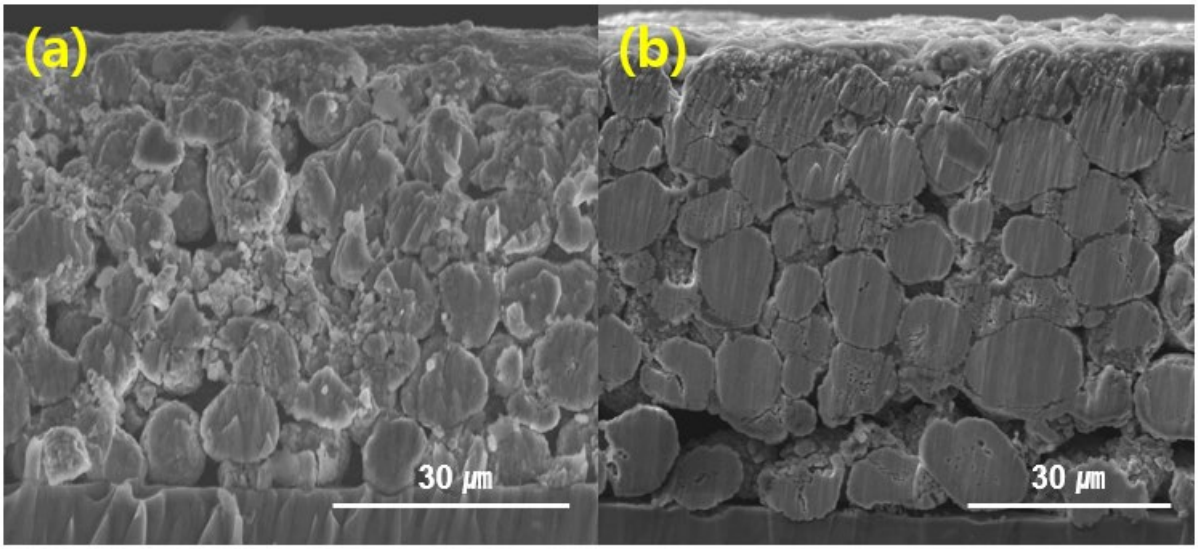

Figure 28. SEM images of cathodes cycled 80 times with (a) 3% $LiNO_3$ and (b) 3% $LiNO_3$+3% $LiPF_6$.

3.6. Effect of $LiPF_6$ and $LiNO_3$ on Li metal anode.

It is shown that $LiNO_3$ + $LiPF_6$ can increase the Li reversibility in Li|Li, Li|Cu and full cells (NCM|Li and NCM|Cu). To analyze the chemical composition of SEI layer, XPS analysis was conducted on Li metal of the NCM|Li full cells after precycle and 3 cycles with 0.5C-rate (**Figure 29).** It is shown that decomposition of DME and LiFSI was suppressed as $LiPF_6$ additives are added more. However, unlike the cathode interphase, $LiPF_6$ could not form enough LiF instead of LiFSI during reductive decomposition. In addition, the formation of ionic conductive Li_3N also decreased because decomposition of LiFSI salt decreased. It means that $LiPF_6$ cannot fully substitute the role of LiFSI in forming SEI layer, so the controlling the amount of $LiPF_6$ additive is important to optimize the SEI layer and Li reversibility. Since 3% $LiNO_3$ + 1.5% $LiPF_6$ showed the balanced SEI components, it could optimize the Li reversibility in the cells.

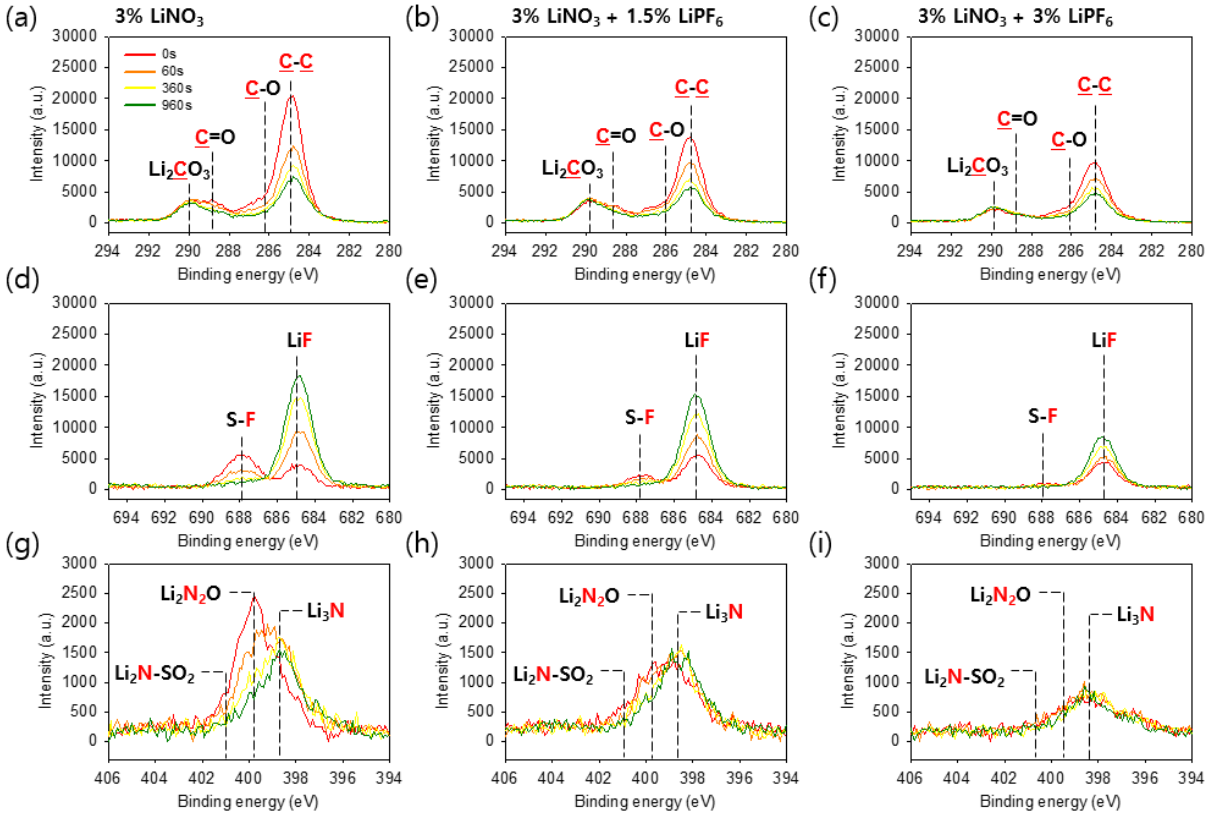

Figure 29. C 1s depth XPS from 0s to 960s of Li metal cycled with (a) 3% $LiNO_3$, (b) 3% $LiNO_3$ + 1.5% $LiPF_6$, (c) 3% $LiNO_3$ + 3% $LiPF_6$. F 1s depth XPS spectra of Li metal cycled with (d) 3% $LiNO_3$, (e) 3% $LiNO_3$ + 1.5% $LiPF_6$, (f) 3% $LiNO_3$ + 3% $LiPF_6$. N 1s depth XPS spectra of Li metal cycled with (g) 3% $LiNO_3$, (h) 3% $LiNO_3$ + 1.5% $LiPF_6$, (i) 3% $LiNO_3$ + 3% $LiPF_6$. Li metals are precycled with 0.1C-rate and cycled 3times with 0.5C-rate in NCM|Li cells at 25°C.

The SEI structure of the $LiNO_3$ + $LiPF_6$ electrolyte was analyzed more with TOF-SIMS analysis. In **Figure 30**, it is shown that the organic layer formed by decomposition of DME solvent in 3% $LiNO_3$ electrolyte is thicker than that of 3% $LiNO_3$ + 1.5% $LiPF_6$ electrolyte. In addition, LiF_2^-, SO^- and SF^- peaks which mean LiFSI salt decomposition decreased sharply inside the SEI layer in 3% $LiNO_3$ + 1.5% $LiPF_6$ electrolyte compared to 3% $LiNO_3$. It means that $LiNO_3$ + $LiPF_6$ could efficiently suppress the decomposition of salt and organic solvent, forming thin and inorganic based SEI layer.

Figure 31 shows the surface and cross-section of Li metal anodes which were retrieved after precycle in NCM|Li full cells with each electrolyte. It can be found that Li metal is corroded in no additive electrolytes with dendritic irreversible Li layer while $LiPF_6$ shows particle-like Li morphology and $LiNO_3$ shows partially formed irreversible Li layer with dense Li morphology. The electrolytes using combination of $LiPF_6$ and $LiNO_3$ shows that there is almost no Li corrosion and no irreversible Li layer. However, the Li metal 3% $LiNO_3$ + 3% $LiPF_6$ electrolyte has uneven Li surface and it is assumed that Li was unevenly plated and stripped because of low contents of ionic conductive Li_3N component in the SEI layer.

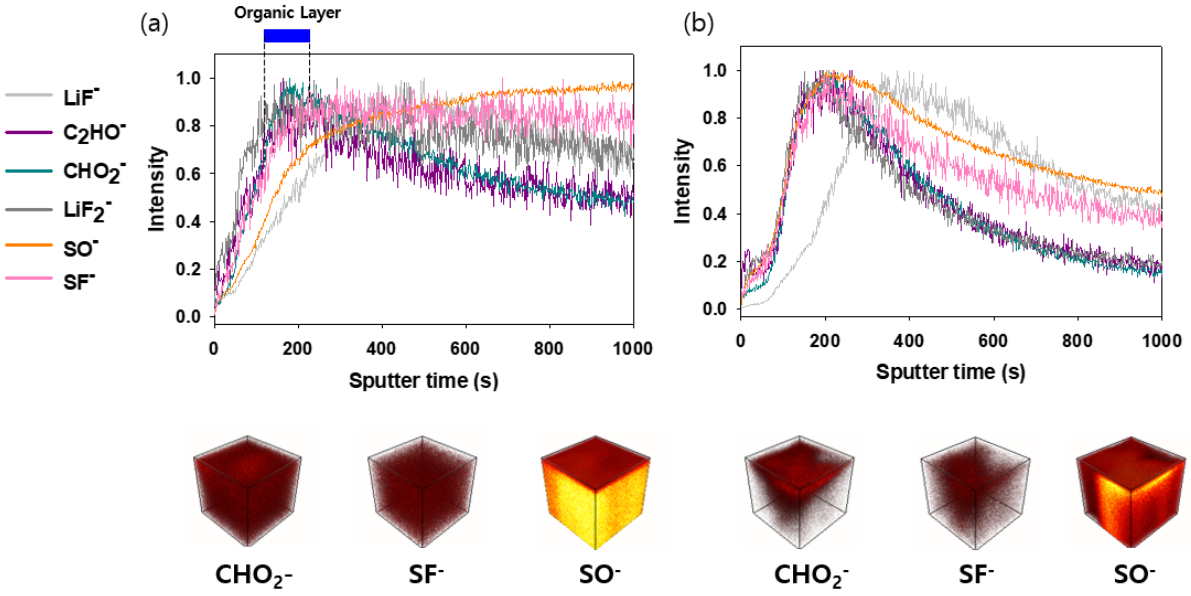

Figure 30. TOF-SIMS analysis on Li metal anode cycled 40 times in NCM811|Li full cells with 0.9C-rate at 25°C. (a) 2M LiFSI DME + 3% $LiNO_3$, (b) 2M LiFSI DME + 3% $LiNO_3$ + 1.5% $LiPF_6$

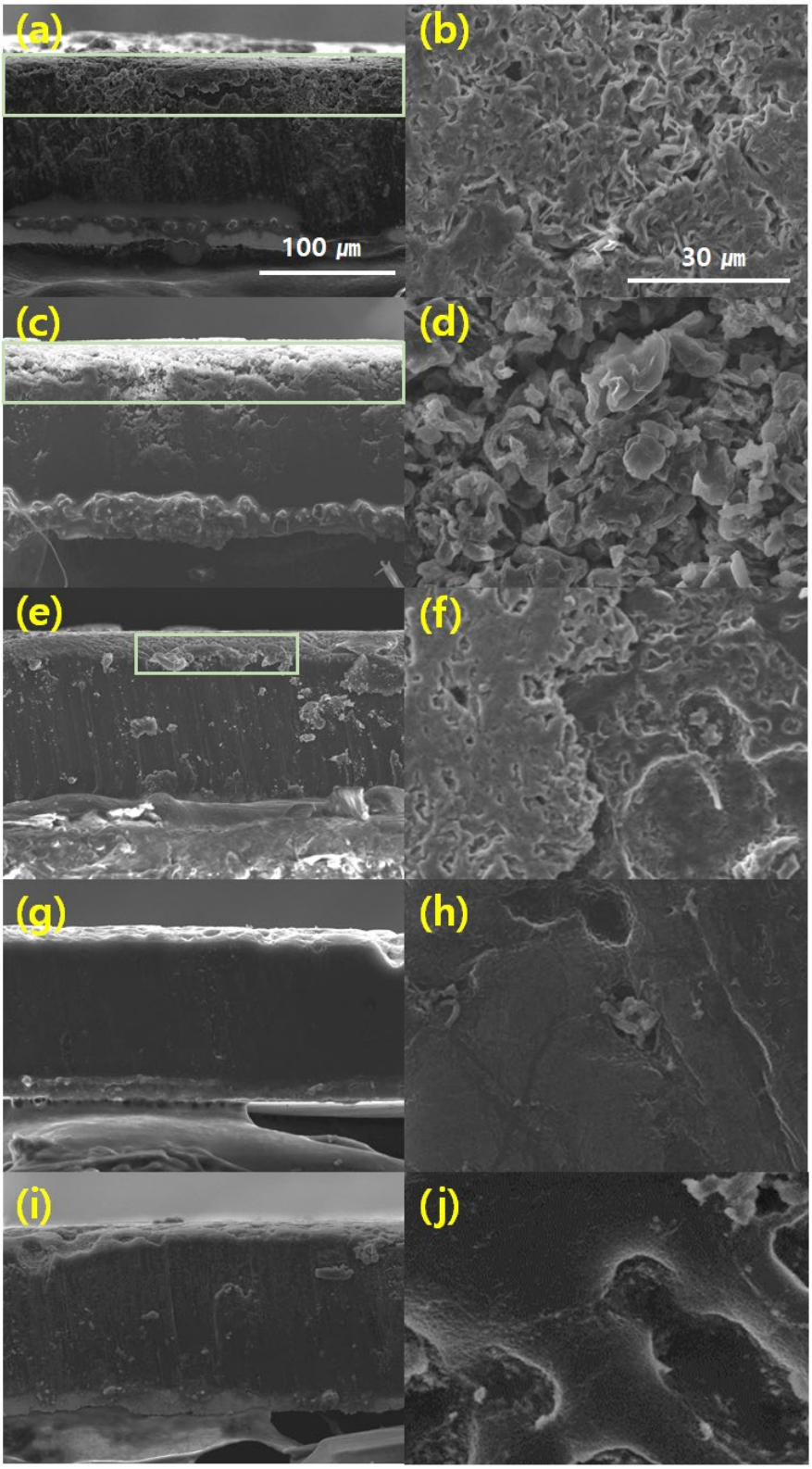

Figure 31. SEM images of Li metal anode retrieved after precycle with each electrolyte in NCM811|Li. (a), (b) No additive, (c), (d) 1.5% $LiPF_6$, (e), (f) 3% $LiNO_3$, (g), (h) 3% $LiNO_3$ + 1.5% $LiPF_6$, (i), (j) 3% $LiNO_3$ + 3% $LiPF_6$.

4. Conclusion

In this paper, we verified that combination of LiF-forming $LiPF_6$ additive and Li_3N forming $LiNO_3$ additive can improve the cycle performance of the Li metal batteries with high energy densities and we demonstrated how the $LiNO_3$ and $LiPF_6$ can form stable SEI and CEI layer on both electrode and improve reversibility of each electrode. Especially, the combination of $LiPF_6$ and $LiNO_3$ showed that it can improve reversibility of Li metal so we can use thin Li metal (less excess Li) for development of high energy density batteries. With XPS and TOF-SIMS it was shown that more addition of $LiPF_6$ could improve performance of the cathode in the cells as it suppressed the decomposition of salt and solvent and formed enough inorganic LiF-based CEI, but it could degrade the reversibility of Li when the addition of $LiPF_6$ was too much so optimization of $LiPF_6$ content is necessary for the best performance of the full cell. Based on this understanding of how $LiPF_6$ affect the CEI and SEI in the LMBs, it is expected that more advanced electrolyte using $LiPF_6$ and $LiNO_3$ will be developed for advanced Li metal batteries.

5. Reference

[1] Y. Liu and Y. Yang, Recent Progress of TiO2-based Anodes for Li Ion Batteries, *Journal of nanomaterials*, 2016, 8123652

[2] D. Liu and G. Cao, Engineering Nanostructured Electrodes and Fabrication of Film Electrodes for Efficient Lithium Ion Intercalation, *Energy Environ. Sci.*, 2010, 3, 1218-1237

[3] K. Parajuly, D. Ternald, R. Kuehr, The Future of Electric Vehicles and Material Resources : A Foresight Brief, 2020, UNU/UNITAR- Scycle (Bonn) & UNEP0IETC (Osaka)

[4] S. chen, F. Dai and M. Cai, Opportunities and Challenges of High-Energy Lithium Metal Batteries for Electric Vehicle Applications, *ACS Energy Lett.*, 2020, 5, 10, 3140–3151

[5] John Emsley, *The Elements* (3rd edition), Oxford: Clarendon Press, 1998

[6] Yaron S. Cohen, Yair Cohen and Doron Aurbach, Micromorphological Studies of Lithium Electrodes in Alkyl Carbonate Solutions Using in Situ Atomic Force Microscopy, *J. Phys. Chem. B*, 2000, 104, 51, 12282-12291

[7] Z. Luo, X. Qiu, C. Liu, S. Li, C. Wang, G. Zou, H. Hou and X. Ji, Interfacial Challenges towards Stable Li Metal Anode, *Nano energy*, 2021, 79, 105507

[8] F. Wu, J. Maier and Y. Yu, Guidelines and Trends for Next Generation Rechargeable Lithium and

Lithium-ion Batteries, *Chem. Soc. Rev.,* 2020, 49, 1569-1614.

[9] K. Liu, Y. Liu, D. Lin, A. Pei and Yi cui, Materials for Lithium-ion Battery Safety, *Science Advances*, 2018, 4, eaas9820s

[10] A. Louli, M. Genovese, R. Weber, S. Hames, E. Logan and J. Dahn, Exploring the Impact of Mechanical Pressure on the Performance of Anode-free Lithium Metal Cells, *Journal of The Electrochemical Society*, 2019, 166, A1291-A1299

[11] Seunghyun Ko, Soon Chang Lee, Chul Wee Lee and Ji Sun Im, A Co-free Layered $LiNi_{0.7}Mn_{0.3}O_2$ Cathode Material for High-energy and Long-life Lithium-ion Batteries, *Journal of Alloys and Compounds*, 2014, 613, 96-101

[12] Seong-Min Bak, E. Hu, Y. Zhou, X. Yu, S. Senanayake, Sung-Jin Cho, Kwang-Bum Kim, Kyung Yoon Chung, X. Yang and Kyung-Wan Nam. Structural Changes and Thermal Stability of Charged $LiNi_xMn_yCo_zO_2$ Cathode Materials Studied by Combined In Situ Time-resolved XRD and Mass Spectroscopy, *ACS Appl. Mater. Interfaces*., 2014, 6, 22594−22601

[13] J. Qian, W. Henderson, Wu Xu, P. Bhattacharya, M. Engelhard, O. Borodin and J. Zhang, High Rate and Stable Cycling of Lithium Metal Anode, *Nature Communications*, 2015, 6, 6362

[14] X. Ren, L. Zou, X. Cao, M. H. Engelhard, W. Liu, S. D. Burton, H. Lee, C. Niu, B. E. Matthews, Z. Zhu, C. Wang, B. W. Arey, J. Xiao, J. Liu, J. -G. Zhang and W. Xu, Enabling High-Voltage Lithium-Metal Batteries under Practical Conditions, *Joule.*, 2019, 3, 1662-1676.

[15] D. Aurbach and E. Granot, The Study of Electrolyte Solutions based on Solvents from the "Glyme" Family (Linear polyethers) for Secondary Li Battery Systems. *Electrochem. Acta*, 1997, 42, 697–718.

[16] S. Jeong, H. Seo, D. Kim, H. Han, J. Kim, Y. Lee, Y. Iriyama, T. Abe and Z. Ogumi, Suppression of Dendritic Lithium Formation by using Concentrated Electrolyte Solutions, *Electrochem. Communication*, 2008, 10, 635–638.

[17] M. Park, S. Ma, D. Lee, D. Im, S. Doo and O, Yamamoto, A Highly Reversible Lithium Metal Anode, *Scientific report*, 2014, 4, 3815–3822.

[18] Y. Lee, T. K. Lee, S. Kim, J. Lee, Y. Ahn, K. Kim, H. Ma, G. Park, S. -M. Lee, S. K. Kwak and N. -S. Choi, Fluorine Incorporated Interface Enhances Cycling Stability of Lithium Metal Batteries with Ni-rich NCM Cathodes, *Nano Energy.*, 2020, 67, 104309.

[19] Y. Dong, N. Zhang, C. Li, Y. Zhang, Y. Wang, M. Jia, Y. Zhao, L. Jiao, F. Cheng and J. Xu, Fire-Retardant Phosphate-Based Electrolytes for High-Performance Lithium Metal Batteries, *ACS Appl. Energy Mater.*, 2019, 2, 2708−2716

[20] S. Chen, J. Zheng, L. Yu, X. Ren, M. H. Engelhard, C. Niu, H. Lee, W. Xu, J. Xiao, J. Liu and J. -G. Zhang, High-Efficiency Lithium Metal Batteries with Fire-Retardant Electrolytes, Joule., 2, 1548-1558.

[21] X. Ren, S. Chen, H. Lee, D. Mei, M. H. Engelhard, S. D. Burton, W. Zhao, J. Zheng, Q. Li, M. S. Ding, M. Schroeder, J. Alvarado, K. Xu, Y. S. Meng, J. Liu, J. Zhang and WuXu, Localized High-Concentration Sulfone Electrolytes for High-Efficiency Lithium-Metal Batteries, *Chem*, 2018, 4, 1877-1892.

[22] X. Zhang, X. Chen, X. Cheng, Bo. Li, X. Shen, C. Yan, J. Huang and Q. Zhang, Highly Stable Lithium Metal Batteries Enabled by Regulating the Solvation of Lithium Ions in Nonaqueous Electrolytes, *Angew. Chem.*, 2018, 130, 5399 –5403,

[23] Z. Brown, S. Heiskanen and B. L. Lucht, Using Triethyl Phosphate to Increase the Solubility of LiNO3 in Carbonate Electrolytes for Improving the Performance of the Lithium Metal Anode, *J. Electrochem. Soc.*, 2019, 166, A2523

[24] T. Ma, G. Xu, Y. Li, Li Wang, X. He, J. Zheng, J. Liu, M. H. Engelhard, P. Zapol, L. A. Curtiss, J. Jorne, K. Amine and Z. Chen, Revisiting the Corrosion of the Aluminum Current Collector in Lithium-Ion Batteries, *J. Phys. Chem. Lett*. 2017, 8, 1072−1077,

[25] X. Wang, E. Yasukawa and S. Mori, Inhibition of Anodic Corrosion of Aluminum Cathode Current Collector on Recharging in Lithium Imide Electrolytes, *Electrochimica Acta*, 2000, 45, 2677–2684,

[26] D. P. Wikinson, H. Blom, K. Brandt, D. Wainwright, Effects of Physical Constraints on Li Cyclability, *Journal of Power Sources*, 1991, 36, 517-527

[27] S. Li, Q. Liu, W. Zhang, L. Fan, X. Wang, Z. Shen, X. Zang, Yu. Zhao, F. Ma and Y. Lu, High-Efficacy and Polymeric Solid-Electrolyte Interphase for Closely Packed Li Electrodeposition, *Advanced science*, 2021, 8, 2003240

[28] M. Genovese, A. J. Louli, R. Weber, S. Hames and J. R. Dahn, Measuring the Coulombic Efficiency of Lithium Metal Cycling in Anode-Free Lithium Metal Batteries, *Journal of The Electrochemical Society,* 2018, 165, A3321-A3325.

[29] H. Wang and K. Xie, Investigation of Oxygen Reduction Chemistry in Ether and Carbonate Based Electrolytes for Li-O_2 Batteries, *Electrochemica Acta.*, 2012, 64, 29-34.

[30] Lucas Lodovico, A. Varzi and S. Passerini, Radical Decomposition of Ether-Based Electrolytes for Li-S Batteries, *Journal of The Electrochemical Society,* 2017, 164, A1812-A1819